UNIVERSITY OF GAZIANTEP

GRADUATE SCHOOL OF

NATURAL & APPLIED SCIENCES

CHARACTERISTICS OF THE BORON DOPED CdSe FILMS

DEPOSITED BY SPRAY PYROLYSIS METHOD

M.Sc. THESIS

IN

ENGINEERING OF PHYSICS

BY

DARYA RASUL AHMED

JANUARY 2017

Characteristics of the Boron Doped CdSe Films

Deposited by Spray Pyrolysis Method

M.Sc. Thesis

in

Engineering of Physics

University of Gaziantep

Supervisor

Prof. Dr. Metin BEDİR

Co-Supervisor

Assist Prof. Dr. Serap ÇELİK

By

Darya Rasul AHMED

January 2017

REPUBLIC OF TURKEY

UNIVERSITY OF GAZİANTEP

GRADUATE SCHOOL OF NATURAL & APPLIED SCIENCES

ENGINEERING OF PHYSICS

Name of the thesis: Characteristics of the Boron Doped CdSe Films Deposited by Spray
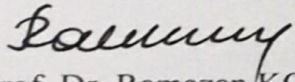Pyrolysis Method

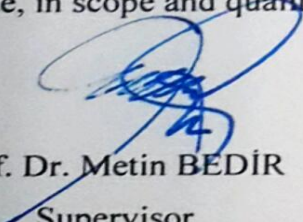Name of the student: Darya Rasul AHMED

Exam date: 23 January 2017

Approval of the Graduate School of Natural and Applied Sciences
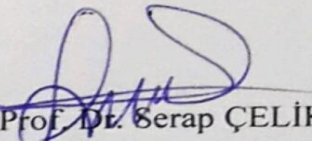
Prof. Dr. A. Necmeddin YAZICI

Director

I certify that this thesis satisfies all the requirements as a thesis for the degree of Master
of Science.

Prof. Dr. Ramazan KOÇ

Head of Department

This is to certify that we have read this thesis and that in our consensus opinion it is fully
adequate, in scope and quality, as a thesis for the degree of Master of Science.

Prof. Dr. Metin BEDİR

Supervisor
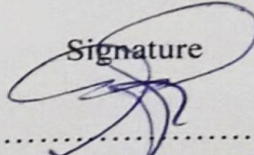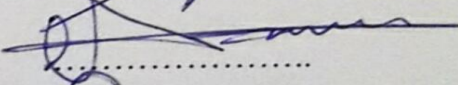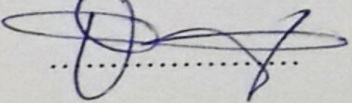
Assist. Prof. Dr. Serap ÇELİK

Co-Supervisor

Examining Committee Members: Signature

Prof. Dr. Metin BEDIR   ....

Assoc. Prof. Dr. Huseyin TOKTAMIS   ....

Assist. Prof. Dr. Rasim ÖZDEMIR   ....

I hereby declare that all information in this document has been obtained and presented in accordance with academic rules and ethical conduct. I also declare that, as required by these rules and conduct, I have fully cited and referenced all material and results that are not original to this work.

Darya Rasul AHMED

ABSTRACT

CHARACTERISTICS OF THE BORON DOPED CdSe FILMS DEPOSITED BY SPRAY PYROLYSIS METHOD

AHMED Darya Rasul
M.Sc. in Department of Engineering Physics
Supervisor: Prof. Dr. Metin BEDİR
Co-Supervisor: Assist.Prof.Dr. Serap ÇELİK
January 2017, (76) pages

In this study, Boron doped CdSe films were deposited by spray pyrolysis under different deposition conditions. The influence of the preparation technique on the structural, morphological and optical properties of the Boron doped CdSe films were investigated by using X-ray diffraction (XRD), SEM analysis and optical transmission. The optical properties of the films were investigated from optical absorption coefficient and transmittance spectra data using double beam visible spectrophotometer. Boron doped CdSe films were prepared by spray pyrolysis technique at 275^0C substrate temperature, which is using boric acid (H_3BO_3) as dopant source, and their properties were investigated as a function of doping concentration. Boron doping was achieved by adding 0.0025 M, 0.010 M, 0.015 M, 0.05 M. H_3BO_3 to the starting solution. The crystal structure of the films was studied by X-ray diffraction with Cu-K$_\alpha$ radiation (1.5406 ^{o}A). The range of 2θ angle was from 20° to 80°. X-ray analysis showed that the films were polycrystalline fitting well with a cubic structure and have preferred orientation in the diffraction lines produced by the (100), (002), (101), (200)$_{CdO}$, (103), (202), (210) and (300) planes of hexagonal (wurtzite) structure of CdSe, respectively. Optical band gap of the undoped and B-doped CdSe films were found to vary from 1.74 to 2.17 eV. The changes observed in the energy band gap and structural properties of the films related to the boric acid concentration are discussed in detail.

Key words: CdSe films, Boron-doping, X-ray diffraction, Optical absorption.

ÖZET

SPRAY PYROLIZ METODUYLA BÜYÜTÜLEN BOR KATKILI CdSe FILMLERIN KAREKTERIZASYONU

AHMED Darya Rasul
Yüksek Lisans Tezi
Fizik Mühendisliği Bölümü
Danışman: Prof. Dr. Metin BEDİR
Yardımcı Tez Danışmanı:Yrd.Doç.Dr.Serap ÇELİK
Ocak 2017, (76) sayfa

Bu çalışmada, değişik depolama şartları altında spray pyrolsiz methodu ile bor katkılı CdSe filmleri elde edilmiştir. Değişik hazırlama tekniklerinin boron katkılı CdSe filmlerin yapısal, morfolojik ve optiksel özelliklerine etkisi X-ışını kırınımı (XRD), SEM analizi ve optik geçirgenlik metotları kullanılarak incelenmiştir. Çift ışınlı görünür spektrometreyle elde edilen optik absorbans katsayısı ve geçirgenlik spektrumu datalarıyla filmlerin optiksel özellikleri incelendi. Bor Katkılı CdSe filmler 275^0C altlık sıcaklığında, katkılama için borik asit (H_3BO_3) kullanılarak spray pyrolsiz tekniği ile hazırlanmıştır ve katkılama konsentrasyonun film özelliklerine etkisi incelenmiştir. Bor katkılaması başlangıç solüsyonuna 0.0025 M, 0.010 M, 0.015 M, 0.05 M. oranlarında H_3BO_3 eklenerek sağlanmıştır. Filmlerin kristal yapı özellikleri Cu-K$_\alpha$ (1.5406 ^{o}A) radyasyonlu X-ışını kırınım ile incelenmiştir. 2θ açısı 20° den 80° ye aralığındadır.X-ışını analizi, filmlerin sırasıyla (100), (002), (101), (200)$_{CdO}$, (103), (202) düzlemlerinde kübik yapılı polikristaller olduğu ve (300) düzlemi için de hekzagonal yapının yönlendirmelerine sahip göstermiştir. Katkılı ve katkısız CdSe fimlerin optik bant aralıkları 1.74 ile 2.17 eV arasında değişmektedir. Filmlerin yapısal özelliklerinin ve enerji bant aralıklarının borik asit konsentrasyonuna bağlı değişimi ayrıntılı olarak incelenmiştir.

Anahtar kelime: CdSe filmler, Bor-katkısı, X-ışını difraksiyonu, Optiksel yutma.

DEDICATION

To my mom for her endless love, support and encouragement throughout my life and all my family they have been a source of unlimited love, friendship, laughter, support, and motivation.

ACKNOWLEDGEMENTS

TABLE OF CONTENTS

Pages

LIST OF FIGURES

Pages

LIST OF TABLES

CHAPTER 1

Literature Survey

1.1 Introduction

Thin films are widely used as protection to avoid corrosion, to resist, in optical applications, like sensors and electrical devices likewise thermal barriers. Thin films deposited different ways; spray pyrolysis, chemical bath deposition, pulsed laser epitaxy, chemical vapor deposition, electron beam, etc. The simplest and easy way to make these thin films is the spray pyrolysis. With this technique, a lot of advantages can be taken because it is a coating technique for the produce films, and also the instrument is very simple, the method is strong if it used properly controlled, a very high quality film will be produced with a low cost as oxide films, when the substrates are put under heating there will be oxide layers directly from the substrate surface on the pyrolysis with very homogeneous layers on the substrate very good adhering is expected. The determination of the caution composition of the deposited layers is done only by the composition of the precursor solution [1].

In preparing thick and thin films, coatings, and powders the technique which is being used in the Spray pyrolysis. Spray pyrolysis if differ from the other film deposition, which is because it provides an ordinary and nearly very low cost process method particularly according to equipment costs. Spray pyrolysis provides a simple way to producing films of any constitution. It doesn't need a very high sort of substrate or chemicals for dense and porous films. This method is worked and also for powder productions. Different kinds of layered films are prepared by using this technique. In the

industry of glasses Spray paralysis is being used for many years [2] and also in the production of solar cell [3]. Spray pyrolysis device is an equipment which is constituted of an atomizer, precursor solution, substrate heater, and controlling of temperature. Some researcher used air blast as an atomizers [4], someone used ultrasonic raditions [5] and some of them used electrostatic methods [6].

1.2 Literature Survey

There are many kinds of published spray pyrolysis techniques. The revision has made by Mooney and Radding of spray pyrolysis method, and reviewed the importance of deposited films with specific films such as (especially CdS), and new application [7]. Garcia and Tomar talked about the ways of preparing and the importance of sprayed films, application in anti-reflection coatings, gas sensors and solar cells [8]. Albin and Risbud explained the tools, the process and optoelectronic materials deposited by the technique spray pyrolys [9]. Pamplin has published a reviewed of spraying solar cell materials and its technique bibliography of references [10]. Patil reviewed the techniques of different atomization with thin metal oxide and chalcogenide films by spray pyrolysis [11]. Gauckler and Bohac have details about the way of chemical spray deposition and introduced more or less models of sprayed YSZ films [12]. Sprayed film presented in this review. Same examples of the impact of deposition temperature, the harbinger solution on film construction and properties was explained. Spray pyrolysis thin-film models was also showed. Danius Perednis & Ludwig J. Gaucher reviewed spray pyrolysis it is habile and impact technique to deposit metal oxide films. The Film's quality and property rely on process parameters. The temperature under layer surface is the most important parameter, the film will be as rough and porous as the substrate temperature higher. The film will be broken if the temperatures was very little. The crystallinity likewise depends on the deposition temperature and another physical property of the deposited films. Most important spray parameter is precursor solution. That impacts the morphology and the deposited film properties. Various additives in precursor solution can change the morphology and properties of films. It is said that the CVD modifier process situated near the surface of the substrate. Although, some clarifications dispute the involvement of a process for a CVD feature. More endeavor will be needed to show the process for deposited films [13].

Many researcher pay much attention to the thin films of II-VI compound semiconductors due to their enforcement in the solid-state physics. These group of the semiconductors the band gap is about 1-3 eV in the visual zone and it is a common in the world of optoelectronic instrument. One of the most common semiconductor materials is Cadmium selenide (CdSe) in this group and during these years the physical properties of both essential and workable purpose have actually researched. It is initial importance crate the equipment fixed for several important applications in the many solid-state tools like electron beam pumped lasers, light-emitting diodes, electroluminescent devices, solar cells, and high-efficiency thin film transistors, etc. [14]. CdSe is the commonest researched semiconductor widely utilized as photoanode in photoelectrochemical cells (PECs) and photoconductive cells. 16.7% of energy change efficiency has known with individual single crystal photo anodes by adding electrolyte modification [15]. More effective photoconductors it has been invented with a screen printing and chemical bath deposition [16,17]. Techniques like a vacuum evaporation [18] and electrodeposition [19] it has been used for the making of thin cadmium selenide films. Also, the method of spray-pyrolysis was applied long ago to make cadmium selenide films, toxic cyanide/selenourea were added as selenium provenance by K.R. Murali and T. Elango. They studied that the chemically deposited CdSe thin film by adding non-toxic selenosulfate as the selenium provenance. The substrate temperature was difference in about from 300°C to 500°C. They used the methods; X-ray diffraction (XRD), photoconductivity measurements and optical absorption to characterization of the films.Single-phase hexagonal CdSe thin films are characteristic by XRD patterns. Resistivity of the produced films was discovered in about (10 - 120 MV) rely on the substrate temperature. A direct band gap of 1.65 eV was gained by optical analysis. The photosensitivity range is about 3500 at a substrate temperature of 450°C [20].

Ashok U. Ubale and Syed Ghause Ibrahim declared that, the nanocrystalline of thin films ($Cd_{1-x}Fe_xSe$) are actually deposited onto glass substrates at temperature 573 K from watery resolutions of FeCl, CdCl and selenium powder adding the chemical spray technique. The structural, morphological, optical characterizations, compositional and electrical were executed using X-ray diffractometry (XRD), (SEM), (EDAX), (AFM), resistivity and optical absorption measurement techniques. The deposited ($Cd_{1-x}Fe_xSe$) thin film is nanocrystalline in natural with hexagonal lattice. The band gap of optical

Cadmium selenium thin film was of request 1.85 eV and it increase with the compositional parameter 'x' and it will be 2.60 eV for FeSe thin film. The electrical resistivity of ($Cd_{1-x}Fe_xSe$) thin film was request 10^6 Ω.cm and declare relation rely in 'x'. The thermo-emf measurements are assured that N-type conductivity ($Cd_{1-x}Fe_xSe$) thin films [21]. P. Soundarrajan and T. Logu, K. Sankarasu Bramanian was studied the chemically sprayed CdSe thin film onto glass substrates at substrate temperature 200°C. The deposition film was heated in air atmosphere in about 3 hours, in the various temperature (350, 450°C). The deposition films have the same crystalline sphalerite cubic structure and their optical band gap is E_g = 2.4 eV. They said that after heating, semi-stable cubic sphalerite phase converts into good stable crystal hexagonal wurtzite phase. It is reported that the optical band gap of CdSe was decreased from 2.4 eV to 1.75 eV. The face rudeness rate was 1.5 nm of the deposition films it will becomes into 4.2 nm after heating the films by air atmosphere. The reached corner is shown to change of (94° ± 1° to 81° ± 1°) with high temperatures on it. Moreover, from Wenzel's declaration it was found that Cadmium Selenium thin films is hydrophilic in nature [22].

T. Logu, et al. impact of antimony (Sb) in CdSe thin films has been inspected. Pristine and Sb doped Cadmium Selenium thin film it has been deposition via using homemade chemical spray pyrolysis unit. Two films have been discovered to be polycrystalline in nature and have cubic sphalerite structure. Sb doped CdSe films have enlarged a red shift (52 nm red shift for 10% wt Sb) different from pure CdSe film. The decrease of average crystallite size and increase of average surface rudeness has been observed with Sb adding into the host CdSe thin films. Angles of water has discovered to increase from 77.33° to 123.74°, which displayed that the face wettability of the CdSe thin film was varied from hydrophilic to hydrophobic nature by the antimony [23]. R.I. Chowdhury1, M.S. Islam1 studied the (CdSe) thin film have deposition on glass/conducting glass substrates by low-price electro deposition mode. (XRD) mechanism utilizes to determine the steps of occur in the deposition film and noticed that the deposited films were almost made of Cadmium Selenium steps. The (PEC) cell measure show that the Cadmium Selenium film was n-type in electro conductive and optical absorption measurement clarified that the band gap for deposition films was considered that 2.1 eV. The band gap of Cadmium Selenium films was decrease to 1.8 eV when the temperatures come to 723 K in 30 min on air. The face morphological from the deposition film has

been describe via (SEM) and noticed that very similar and regular Cadmium Selenium films was mature at FTO/glass substrates. With n-type Cadmium Selenium windows material in Cadmium Titanium depended solar cell structure [24]. CdSe has produced in these years due to its potential technology important. The composition both of metals chalcogenide of group II-VI semi-conductors in a nano-crystalline form has been quickly grow field of study because of their importance nonlinear optical characteristics, luminescent characteristics, quantum size impact and another importance physical properties and chemical properties [25]. Cadmium Selenium has band gap 1.7 eV so that its convenient to solar energy transformation together with a photovoltaic cell, which was suitable for the spectrum of sunlight [26]. The best optical characteristics made them acceptable for the manufacture for solar cells. In contemporary effort spray pyrolysis mechanism was succeeded employ to made Cadmium Selenium thin film via ordinary and low cost chemical spray pyrolysis mechanism. The films have been describing by (XRD) and UV-VIS optical measure mechanisms. M.M. Betkar, G.D. Bagde was viewed that, the Cadmium Selenium thin film have been deposition on glass substrate in watery resolution via spray pyrolysis mechanism at increase substrate temperatures. In the experimental the CdSe thin films were increasing the temperature of (240, 260, 280, 300, and 320) ℃ employ spray pyrolysis mechanism. The impact of substrate temperatures in structural characteristic was improved. The structural, optical and electrical properties of deposition film were calculated through (XRD), UV-VIS spectroscopy. The XRD (X-Ray diffraction) spectra viewed that the film is on the shape of hexagon in structure. Varied structural parameters like grain size of the films are discovered changed temperature from (240 to 320) ℃ [27].

Y.G. Gudage was studied the electro synthesize method to obtain (CdSe) thin film. A special substrate was used that well-cleaned stainless steel and fluorine doped tin oxide (FTO) covered glass (10-15 Ω/cm^2). XRD research shows that (111) cubic structure with direct band gap. The structural parameters are studied and they are discovered to be rely on the pH of the deposition bath. Energy Dispersive Spectroscopy analyses improve that almost stoichiometric formation of the films deposition of pH 2.70. Atomic Force Microscopy analyses viewed homogenity of deposited on the films. The optical research shows the optical energy gaps discovered in the range of 1.87 to 2.04 eV rely with pH of the chemical bath deposition. Photo luminescence (PL) spectra give blue change in

PL peak location and decrease in luminescence intensity for the films located at pH other than 2.70 [28].

E.U. Masumdar, A.A. Yadav and M.A. Barote, was explained that (CdSe) thin film have been deposition onto good clean glass substrate at various substrates temperature using spray pyrolysis. Aqueous resolutions contain predecessor of Cadmium and selenide have been use to get better quality thin film. The deposition film was defined with structure, morphology, optic, electric and thermo electric characteristic. (XRD) reviewed that the film was polycrystalline hexagonal crystal structure. Scanning electron microscopy studies show that the grains are orderly for disparate spherical form, diffused on the whole face of the substrate. Atomic force microscopy analysis show orderly deposited of the films according the whole substrates face. Energy Dispersive Spectroscopy analyses prove almost stoichiometric deposited of the thin films at 300°C. In optical studies, the transmission datas of the deposition films was determined to direct allowed using optical energy gaps in about of (1.74 eV to 1.87 eV) relying on the substrate temperatures. The activated energy of the thin films has been founded about of (0.19 eV - 0.27 eV) at low temperatures and (0.36 eV - 0.56 eV) at high temperatures. Semiconducting conduct has been cleared of resistive mensuration. The thermoelectric power measurements show that thin films displayed n-type conductive [29].

Many of scientists worked, and deposited CdSe thin films, due to the CdSe thin films were so popular, other technique is crated to produce CdSe thin films and their conclusions were talked about previously. I. A. Kariper was produce CdSe thin film through chemical bath deposition at 50°C. Transmittance, absorption, optical band gap and refractive index have been studied through UV/VIS, spectrum. The XRD structure properties have been observed in hexagonal. The structure and optical characteristic of cadmium selenide thin film, which have been produced with different PH, were analyzed. SEM analyses have been done; surface analyses of the films were deposited accordingly. Many properties of the films have been varied with pH and these properties have been investigated. Tested pH values were at range 7-10. The optical band gap has been varied with the pH of bath, taking values among 1.76 eV and 2.09 eV. And film thickness was measured as 74.65, 106.39, 107.95 and 138.15 nm for the films produces at PH: 7, 8, 9 and 10, respectively. [30].

Yuzhao, et al. was talked about the chemical bath deposited (CdSe) nanocrystallite thin with ammonia and triethanolamine (TEA) as complicating agent, CdCl and NaS as the sources of ions. The structural and optical characteristic of cadmium selenide nanocrystallite thin film are investigate as a function of the NaS concentricity or ammonia concentricity in precursors with (XRD) measurement, (TEM), Ultra Violet-visible spectrophotometer measurement, (SEM) and (EDS). The consequence showed that the Cadmium selenide thin films have cubic phase. Each crystallite consists of some nanocrystalline 3-10 nm in crystalline size. An increasing of crystalline size is due to the increasing in ammonia concentricity. The Se/Cd atom ratios of Cadmium selenide thin film at the first time increased and then decreased with an increased in ammonia concentricity or NaS concentricity. When the ammonia concentrations decrease the optical band gap of Cadmium selenide thin film will be increased. The kinetics and reflection technique of the Cadmium selenide nanocrystallite thin film through this deposited [31].

S. Mahato, et al. was cleared that the Cadmium selenide films were synthesized with ordinary electro deposition this correction on indium tin oxide coated glass substrates. The composition thin film is post heat at 200°C, 300°C and 400°C. (XRD) of the thin film clarified at the hexagonal structures by crystalline size <3 nm for the deposition thin film and 3-25 nm for heat thin film. The face morphological from thin film for field emitted (SEM) displayed desirable face. The higher determination (TEM) of a crystalline of the thin films showed lattice fringes which measure lattice spacing of 3.13 Å identical for (002) plane, indicating the lattice contraction impact, because of smaller size from Cadmium selenide nanocrystalline. The computation of optical band gap for Ultra Violet-visible absorption spectra displayed powerful red shift for increasing in crystalline size, discovering to the charge confinem in Cadmium selenide nanocrystalline [32].

A. Purohit, et al. was studied the research on impact of air heating on structure, optic, morphology and electric characteristic from cadmium selenide thin film are over possessed. Thin film has a thickness 810 nm is deposited onto glass and ITO coated glass substrate by thermal evaporation mechanism. The structural, optical and morphological characteristic of films deposited on glass is studied while ITO coated

glass substrates for electric characteristic. The deposition thin film is submitted into thermal heating at air atmosphere at various temperatures 100°C, 200°C & 300°C. It was concluded that the film has cubic phase for best orientation (111) by (XRD) analysis. The grain size was detected in about (27.11 nm-34.03 nm) and cleared to various utilizing air heating. The dislocation density and strain change with heating in about (0.86-1.36) $\times 10^{11}$ cm^{-2} and (0.276 - 0.347) respectively [33].

S. M Hus¸ and M. Parlak was talked about that, the electric, photo-electric, optic and structure analysis of cadmium selenide thin film deposition via thermal and e-beam evaporation mechanism were carried out using measure temperatures accordance (XRD), transmission, photoresponse, conductivity, mobility and photoconductivity under various illumination intensity. So, consequence of the mensuration's, it was cleared that the thin film deposition via the thermal evaporation mechanism have room temperature conductive value approximate three orders of size greater than the ones deposited using e-beam evaporations. Structure analysis clarified that the thin film deposition via both mechanisms for the same growing parameters have a mix structure for the contribution of cubic and hexagonal structure. Both direct band gap values are gain at 1.71 eV and 1.88 eV. Likewise, sublinear and superliner photoconductive manner attached into sensitizing and deficiency levels located on 0.12 eV and 0.28 eV beneath the conduction band was founded. The subsistence of these levels was showed jointly with the valence band splitting by with photoresponse measurement [34].

C D Lokhande and R B Kale was clarified that, the cadmium selenide thin films are deposition on glass substrate with the CBD mechanism at room temperature. The deposition cadmium selenide thin film was red in color and secularly reflectively. The deposition cadmium selenide layer growing for nanocrystalline cubic phase over for several amorphous phase presents, with an optical band gap 'E$_g$' of 2.3 eV and electric resistivities are in the range of 10^5-10^6 Ω cm. The deposition films are heated in air to 673 K from 4 hours and the impact from heating on structure, morphology, optical and electric characteristic is researched. It must note that after annealing, semi-stable of nanocrystallite cubic phase converts for good stable crystalline hexagonal phase and film clear a (red shift) of band gap E$_g$ is about 0.6 eV. After heating, the crystallite size increased from 45A° to 180A°, which consequences in a decreased in electric resistivity.

These varies have been behavior to the crystalline size subordinate characteristics of cadmium selenide semiconductor thin film [35].

Hazim L. Mansour, et al. was defined that the Cd 0.4 Se 0.6 thin film it has been made on a glass substrate by (CBD) mechanism. Atomic force microscopy and X-ray analyses are used into research the impact from thickness difference on face morphological and crystalline. The optical characteristics of thin film are likewise exacted as a function of film thickness, which was observed to be rectified using the increase of films thickness. This can be attribute to the effect that film thicker than 400 nm was under strain line which decrease as the films thickness increase [36].

Boron is one of the metal that used for prepared the thin films, in this study boron acid is used and doped to CdSe and was investigated the optical, morphological and X-ray diffraction pattern to cleared the good orientation. B-doping Cadmium sulfide film are made via (CBD), which was a low-cost and big region mechanism and manifest to a good research into the industrialist of thin films solar cells, with (H_3BO_3) as doping source, and these characteristics are exacted a function from doped concentricity [37]. Cadmium sulfide thin films chemical deposition of the resolutions contains varies impurity recognized as donor kind of doping into Cadmium sulfide (chlorine, iodine, boron and indium) was discussed. The consequence asserted that the electric resistivity of Cadmium sulfide film doping with B and Cl was subordinate on doping level [38]. The B-doping Cadmium sulfide films are made by the SP mechanism. The structural, electrical and optical characteristics from the films are showed as a function of the substrate temperature (T_s) in the 350-450°C range.

M. Bedir, M. Öztas, Hüsniye Kara was discussed that the B-doping Cadmium sulfide film have been deposited using spray pyrolysis technique upon glass substrate temperatures in about of 350°C – 450°C. The impact from substrate temperature (T_s) in the structural, electrical characteristic and optical characteristic of the film are details. The structural characteristic from B-doped Cadmium sulfide film have been inspected using (XRD) mechanism. The (XRD) spectrum demonstrated that B-doped Cadmium sulfide film is polycrystalline and have a hexagonal (wurtzite) structure. Using scanning electoron microscopy analyses, the face morphological of the film is cleared as an impact of the difference of substrate temperatures. The substrate temperature was

straight concerning for the transfer uncovered in the band gap value derived of optical of parameters and the directly band gap values are determined to be in the area of (2.08 eV-2.44 eV). The electrical details demonstrated that the films deposition at the substrate temperatures 400 °C had high transporter concentricity, Hall mobility and minimum resistivity. This resistivity value decrease with increased in temperature up to 400 °C indicating the semiconducting natural of Boron doping Cadmium sulfide film. The structural parameters are studied, correlated with the substrate temperature (T_s). [39].

Hani Khallaf, Guangyu Chai was studies in situation B-doping from Cadmium sulfide using (CBD) is reported. The impact from boron doped on optical characteristic, withal electrical characteristic, crystalline structure, chemical, and morphological from the chemical bath deposited cadmium sulfide film was discussed which boron doped. The resistivity of films is as low as $1.7 \times 10\text{-}2$ Ω cm and a carrier density is as high as 1.91×1019 cm^{-3}. Band gap of boron doped film was decreased as the [B]/[Cd] ratio in the resolution increased. (XRD), micro- Raman spectroscopy and TEM is used for understanding the chemical and morphological from of film are unaffected via boron doped [40].

Ling Ling Yan was cleared that a chain of CdS/Si hetero structures are made over growing B-doped Cadmium sulfide thin film on silicon nanoporous pillar arrangement (Si-NPA) by (CBD) mode. The experimental data show that boron doped cadmium sulfide thin film can be tuned efficiently over control the mole ratio of [B]/[Cd] of the essential chemical bath deposition resolution. The electrical correction and photovoltaic parameters of solution clear potent reliance onto Boron doping concentricity, and the optimal propertice were done to the specimen make for [B]/[Cd] = 0.01. Different for CdS/Si-NPA solar cell without boron doped, an increase over 300 times to energy transformation activity was realized. The technique to the activity increase was atomize based on the impact of the band gap of boron doped CdS/Si-NPA[41]. Recently on Cadmium sulfide thin film deposition via CBD for boric acid (H_3BO_3) as a dopant source [42]. It was discovered that as the B-doping concentricity incremented, the resistive of Cadmium sulfide film frequently decrease and show the low value of Ω.cm. To optimize the heating conditions and to attain the properties needed for CdTe solar cell application, in the research, B-doped Cadmium sulfide film are made by CBD, followed by heating

at difference temperatures and in varies ambients. impacts of heating temperature and ambient on structural, electrical, and optical characteristic from boron-doped Cadmium sulfide film are inspected.

Jae-Hyung Lee was cleared that the impacts of heating on the characteristic of B-oped Cadmium sulfide film made by CBD with boric acid as a dopant source were investigated. These crystalline orientations and the grain size of Cadmium sulfide films appeared into be industriously impacted by the heating ambient. The crystal structures of H_2-annealed films were wurtzite type for a good orientation of the (002) plane and the grain size slightly increased. For samples annealed in N_2 and air, however, the good orientation of the (002) plane disappeared or decreased and the grain size was identical to or smaller than that for H_2 ambient. When annealing in H_2 the dark resistivity becomes decreased and increased further with increasing annealing temperature. For N_2 and air ambient, the dark resistivity was larger than that of the H_2-annealed films and the optical transmittance was less than that of the H_2-annealed films. These results propose that annealing in H_2 ambient was convenient for photovoltaic device application [43].

P.M. Koinkara, D. Yonekura was cleared that, B-doped nanodiamond (NCD) film are composited in silicon substrate by microwave plasma chemical vapor deposition (MPCVD) mechanism. Impact of space heating on the area emission properties of NCD film has been accurate. The face morphological and quality of film was described by (RS) and (SEM). The scanning electron microscope picture obviously check forming of nanocrystalline diamond (NCD) on the full substrate face. The Raman spectra of the as composited film and film heated at various temperatures in space cleared, the properties peaks at ~1140, 1350 and 1480 cm^{-1} asserting the nanocrystalline natural of the diamond crystalline. The area emission properties of NCD films are reinforce via the fast heating operation. Sill field of thermic treated boron doping NCD films are cleared to be low as likened to growing. The reinforce area emission characteristic perhaps attributed to the atomic flaw make because of heating, which play effective role in the emission technique [44].

X JHao, et al, was cleared that the doping mechanism of Si is used for all-Si tandem solar cells applications. They produced B-doped Si nanocrystals by co-sputtering method. The X-ray photoelectron spectroscopy results change in range Si-B (187 eV)

and/or B-B (188 eV). The change in the constitutional and optical characteristics on the impacts of the boron content on Si quantum dot is analyzed. And the results demonstrate that the boron content increase, the nanocrystal size was a little decreased and the Si crystalline was pressed again. The PL density of the film is decrease as the boron component increased. It was because of B cause flaw and Auger operation induces via efficient doped. These consequences could supply best status into come future Si quantum dot stands on solar cells [45].

Wang Li and Yingyi Li was discussed that in order for thin films solar cell to have higher transformation competence, their front electrodes have to higher electrical conductive and optical impressionability. The front electrode is prepared from diaphanous conductivity oxide film. This study, B-doped ZnO film are growing via the small pressures of (CVD) mechanism and they are using as the front electrode for amorphous silicon thin films solar cell. The growing B-doped ZnO film have well optical characteristic, but their electrical characteristic withal necessity to improvement to enforcement in thin films solar cell. Their studies showed that the electrical characteristic from the growing B-doped ZnO film could be significant reinforced via heating in hydrogen atmosphere, and meanwhile their well optical characteristic are preserved. The process of heated B-doped ZnO film in amorphous silicon thin films solar cell [46].

V.D. Novruzov was showed that the B-doped Cadmium sulfide thin films deposited by spray pyrolysis. The impact of UV light on the structural, optical properties and electrical properties of Boron doped Cadmium sulfide thin film are exacted as a function of boron doping. It is concluded that all specimen is polycrystalline and they have hexagonal structure. It's founded that the excellent direction of non-illuminate specimen exchanges from (101) to (002) with boron composition. The c lattice constant of film decreased of $6.810°A$ for $6.661A^o$ with B-doping. X-ray diffraction peaks density increase for the illuminate with almost all the specimen. The lattice parameter from Boron doped specimen stayed almost constant next illuminate. This stabilization next the illumination of ultra violet light is determined by the optical analysis, photoluminescence studies, electrical analysis of the Boron doped films. The

photoelectrical parameters of Boron doped solar cell are additional strong against the Ultra Violet light [47].

Jaehyeong Lee was discussed that the B-doped Cadmium sulfide thin film are chemical deposition into glass substrate. (XRD), (PL), and Raman mechanism are used for evaluation the quality of Boron doped cadmium sulfide thin film. X-ray diffraction consequence have assured that boron doped cadmium sulfide film have a hexagonal structure in the direction of the (002) plane. The grain size is decreased, but no exchange of the microstructures is noticed. The photoluminescence spectrum for all specimen consist of two bands approximate (2.3 eV) and (1.6 eV) in the region green and red recpectively[48].

CHAPTER 2

THEORY

2.1 Crystal Structure of Semiconductors

Crystalline solid from the fact characterized by the atom formation the crystal arrangement of periodical manner. That is, several fundamental arrangements of atoms that are recurrent in all the solid parts of the whole. Consequently, the crystal seems punctually the same at one point as it does at a series from another equalist point, once the basic periodicity was founded. But, not all solid is crystal [49]. The periodicity of the crystal is described as a condition of the uniform arrangement of point in space called a lattice. It will have added atom at any lattice point in a configuration called a fundamental, which could be one or several atoms possess the same locative order to get the crystal. All situations, the lattice condition a size or cell that performs the perfect lattice and regular recurrent anywhere the crystal. Single crystal, polycrystalline and amorphous, are the three universal kinds of solids according to their atom arrangement. Any kind is properties by the volume of a required area during the material. A required area was located size in which atom or molecular has a uniform geometrical arrangement or periodic amorphous material has required only within a small atomic or molecules [50]. However polycrystalline material has a higher grade of order through much atomic or molecular dimension. A significant parameter is the grain size and its value. It could be affected by process step like a heating. Polycrystalline semi-conductors are utilized in inexpensive, have a wide applications in photovoltaics or as a thin films transistors or in MOS diodes. Polycrystalline materials could be invented of amorphous material by heating steps [50]. The single crystal zone is called grains and are discrete of one other by grain boundaries. Single crystal material, typical have a

higher grade of require, or uniform geometric periodicity, over the full size of the materials. The usefulness of a single crystal material is that, in universal, its electrical characteristic is excellent to those of a non-single crystal material, ago grain boundaries tend to degrade the electrical properties Two-dimensional impersonation of single crystal, polycrystalline, and amorphous, materials are shown in Figure 2.1
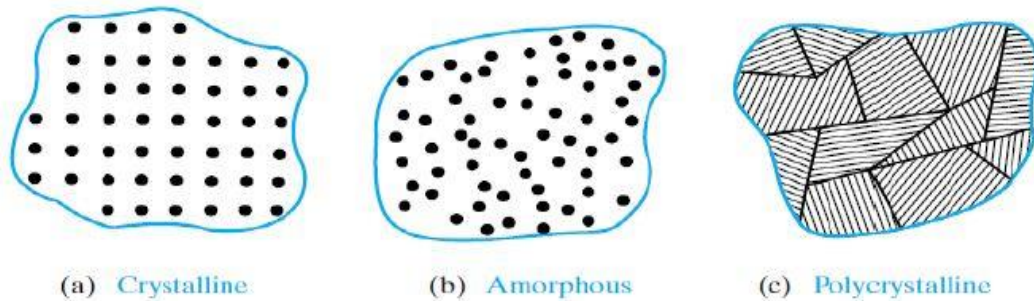
Figure 2.1 (a) Crystalline solids (b) amorphous solids (c) polycrystalline solids [50].

2.1.1 Single crystal

Crystalline solid is a type of solid and has atom which ordered regularly in 3 dimensions. Single crystal has an atomic structural that duplicate periodically across its complete size. Even on unlimited extent scales, any atom is concerning for each other equivalent atom in the structure using transition uniformity, in a single crystal whole views from different points are the same. In single crystal that shown in figure 2.2 the atom array has same order and pattern throughout whole volume. Crystallite Solid is the solid of a material in which the atoms or molecules are in good order in a definite, duplicating pattern in three dimension. Single crystals, typical have a higher grade of order, or regular geometric periodicity, over the entire size of the material.
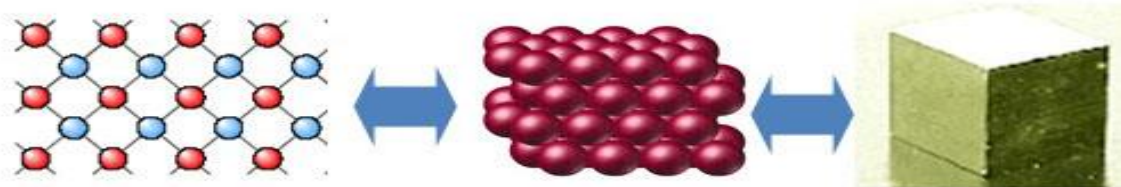
Figure 2.2 Single crystal

2.1.2 Polycrystalline films

Polycrystalline films are usually defined in relations of their grain structure, which is regularly comprehend to contain some measurement of grain size, grain boundary morphological (typical grain form), and film synthesis (distribution of crystallographic orientations). The joining among these properties (size, morphology and synthesis) and process circumstance is understanding qualitatively for mutual low-energy vapor deposited methods connecting relatively clean film materials and substrates for which epitaxial interface formation is not possible. The beginning of epitaxial development is not likely if the substrate is amorphous, of course, and it is improbable if the substrate surface is protected with an adsorbed contaminant layer or if the mismatch strain is too big. In this cases, ad-atoms have a greater tendency for bonding together than for bonding to the substrate. Significant issues in regulatory the structure of a creating thin films is the create flux or deposition rate and the substrate temperature. [51].

Figure 2.3 showing the polycrystalline films, Grain boundaries has an important role when characterization of the polycrystalline semiconductors. These semiconductors perhaps more classified into groups according to size of the grain boundaries such as microcrystalline and nanocrystalline. The grain size of materials can be changed according to the substrate temperature through thin film deposition. And also the thickness of the films can be according to substrate temperature. The electrical resistivity of the films increases according to the attendance of potential barriers on grain boundaries. [51].
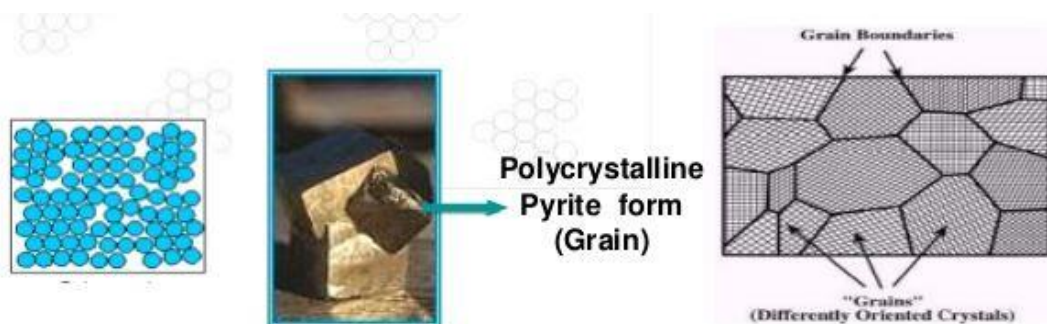
Figure 2.3 Polycrystalline films

Generally, the grain boundaries present allowed levels in the energy gap of a semiconductor and it affects the performance of recombination centers of the minority carriers. It is very important for application of photovoltaic devices. Usually, the conductivity of devices will enhance with increasing grain size. In this context, the larger grain structure results a decrease in resistivity. In order to prevent important grain boundary recombination of electron-hole pairs, it is also the recombinations of e-h pairs are unwanted for photovoltaic applications. The passivation in the grain boundaries affected the device performance, like photovoltaic cells efficiency [52].

2.1.3 Amorphous semiconductors

Amorphous semi-conductors have necessitated enormous area in different devices. These materials could be comparatively a cheap made as the thin film deposition on grade-region substrates. An amorphous solid is called as a solid substance whose atoms arrange apart at equilibrium spacing, but with no long-range periodicity in atom location in its structure. The amorphous structure is as shown in Figure 2.2. Examples of amorphous solids are glass and some types of plastic. Amorphous solids do not show a sharp phase change from solid to liquid at a definite melting point, but rather soften gradually when they are heated [52].
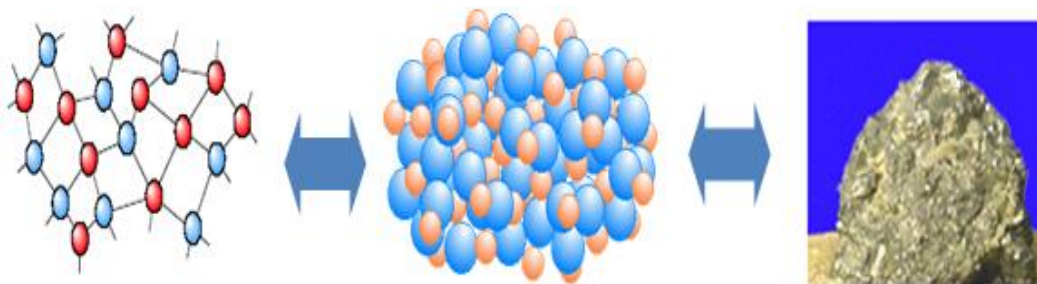
Figure 2.4 Amorphous semiconductors

2.2. Definition of Semiconductors

Semiconductor is a material they are usually a solid, chemical element or compound state. It could behave as an electric conductivity under several conditions and preparing it is a perfect medium to hegemony from electric current. Specific characteristics of the semiconductor rely on the impurities, or dopant materials, added to it. In N-type semiconductors charge carries are negatively-charged electrons. The electrons are used

carrying of the current on a wire. A P-type semiconductors carry current preponderantly as electron insufficiencies which is called as holes. Hole is positive charge. It is similar and opposite into the charge on electron. The semiconductor materials, the flow direction of the holes is opposite to the flow direction of electrons [54]. All of the crystalline elements have capability for conduct electrical current. Their electric conduct The capacity could be controlled selectively using impurity doping materials with boron or aluminum. Semiconductor materials are often used for make solid state electronic devices like transistors, rectifiers, diodes and integrated circuit in the memory chips and computer. Through the last decades, the semiconductor materials are produce in the growth of a wide range of electronic and optical devices which are used in many areas of the technology. The semiconductors material are used in the microelectronic, photovoltaic cells and optoelectronic devices, this developments and implementations have been preserved through a best comprehension of the inter relation among the various side (i.e., characterization of materials, performance, synthesis and processing, structure and properties) of this multi disciplinary area. At this stage, the main advantage of the semiconductor is their electronic band structure which lies between an insulator and conductor. Its clear that the semiconductor possess electric resistance in a domain among these typical metals and insulators. The number of its charge carries may impact the electric conductivity of semiconductors due to change via several requests from magnitude. This varying ability or control on the electrical conductivity on the orders of magnitude in the semiconductor provides the applications in many area, such as electronic applications, like transistors, and various optical devices and as a electro-magnetic radiation detector, as a photonic in fiber optic applications. Current computer technology, which is mainly based on the capacity of transistors to move quickly as the "on" or "off" switch while the light wave communications systems rely on a semiconductor material such as optical sensor. Substantial property and characteristic of the semiconductors are to rely degree heat conductive. When the temperature increases the conductivity in metals decreases but in the semiconductors is differ, the conductivity in the semiconductor increases with increasing temperatures. The substantial parameters predominatingly define a set from semiconductor applications is a certain basic energy gap in the range among 0 eV and about 4 eV into semiconductor. It will be noted however, that the semiconductor limits into each of the resistance between approximately the maximum limit of the energy gap on 4 eV, approximations only. The

semiconductors can be categorized into two groups according to their purity; the first one the examples of semiconductors that are commonly utilized in electronic and optical applications are group IV elemental semiconductors such as Si and Ge, and second one is the compound semiconductors. Group III–V compound such as AlAs, InAs, InSb GaAs, ,GaN, InP, and GaP, group II–VI compounds such as CdS, ZnS, CdSe, ZnSe, ZnTe and CdTe and group IV–VI compounds in examples PbSe, PbS, and PbTe. In addition to these elemental and compound semiconductors, materials made ternary compounds [56].

2.2.1 Intrinsic Semiconduction

Semiconductors in a much pure shape are recognized as an intrinsic semiconductor. Semiconductor perhaps regarded as an intrinsic semiconductor if its thermic produced carrier density (i.e., ni) is greater than the remaining impurity densities or background doping. An intrinsic semiconductor behaves an insulator at $T = 0$ K which means its the conduction band are fully empty and the valence band are totally filled. So there is no conduction between allowed bands. But, when the temperature increase, Electrons in the valence band gain thermal energy and are excited into the conduction band, leaving behind an equal number of holes in the valence band. Also the number of electrons in the conduction band and the number of holes in the valence band are equal to each other in an intrinsic semiconductor. Therefore, the intrinsic carrier density could be expressed by: [53]

$$n_i = n_o = p_o$$

where p_o and n_o mean the intrinsic concentrations of the holes and electrons, respectively. An intrinsic semiconductor, till at normal temperature, hole-electron pairs are produced. Also the second methods for excitation of carriers is applying an electric field. When electric field is applied to the intrinsic semiconductor, also the current conduction happens, specifically; by holes and free electrons as see in Figure (2.5). Free electron is generated due to the separation of some covalent bonds via thermal energy. However, hole is produced in the covalent bonds. Under the influence of electric field, conduction starts in the semiconductor by producing of the free electrons and holes pairs. Then, the total currents in the semiconductors are due to these free electrons and holes pairs. It is perhaps renowned that current in the external wires is completely electronic

by electrons. In Figure 2.5, holes moved to the negative side, electrons moved to the positive side of source [54].
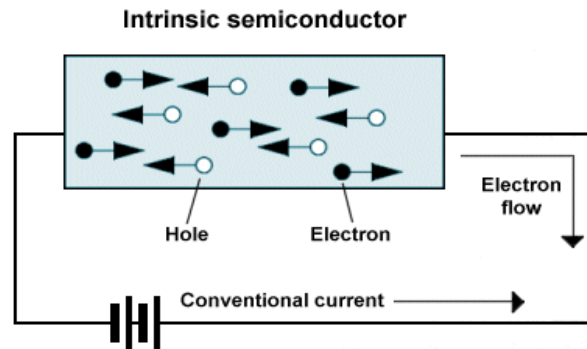
Figure 2.5 Intrinsic semiconductor

In intrinsic semiconductors, each electron excited to the conduction band left behind a missing electron in the valance band. Also an empty electron state is occured in the valence band. Under the effect of an electrical field, the location of empty electron state is started to move. By this method, the missing electron in the valance band accelerated is started to behave as positively charged particle named a hole. Hole has a charge which has the same magnitude but opposite sign with the electron [53].

2.2.2 Extrinsic Semiconduction

Even with the application of thermal energy, only a few covalent bonds are broken in , the intrinsic semiconductor yielding small current conduction ability in the room temperature. A much more efficient method of increasing conduction ability of the semiconductors is by adding very small amounts of selected additives to them. This is satisfied by adding a little amount of opposite impurity to a semiconductor. When these impurities are added to the semiconductor they are called as an extrinsic semiconductor or doped semiconductor. The procedure of addition impurity to a semiconductor are named as doping. The main purpose of semiconductor doping is to increase the conductivity. When a semiconductor is doped, the number of free charges moved by an external applied voltage are increases. Also the electrical properties of a semiconductor can also be changed by doping. The conductivity of semiconductors can be drastically increased by the controlled addition of impurities to the intrinsic semiconductor material. The mobility of both electrons and holes decreases linearly with an increase in temperature, but the number of mobile charge carriers increases exponentially with an

increase in temperature. Furthermore, the conductivity behavior of an extrinsic semiconductor depends on the type of impurity atoms that it has been doped with. There are two types of extrinsic semiconducting; n-type semiconductor shown in Figure 2.6 and p-type semiconductor shown in Figure 2.8.

2.2.3 n-Type Extrinsic Semiconduction

There are two types of dopants, n-type dopants and p-type dopants. N-type dopants are called donors while p-type dopants are called acceptors. The adding of pentavalent impurity satisfies a great number of free electrons by the excess electrons in the semiconductor crystal. Main examples of pentavalent impurities are arsenic and boron like impurities which produced n-type semiconductor because they offer free electrons to the semiconductor crystal. To understand the construction of n-type semiconductor, consider a pure germanium crystal doped by arsenic. A great number of free electrons developed in the crystal by adding dopants as shown in Figure 2.6. It is seen that for every arsenic atom added, one free electron will be available in the germanium crystal.
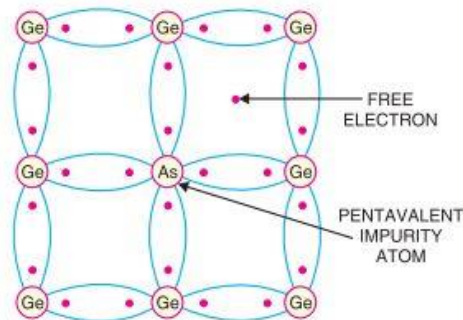
Figure 2.6 N-type extrinsic semiconductor [54]

Figure 2.7 displays the energy band explanation of n-type semiconductor. The adding of pentavalent impurities is generated a great number free electrons in conduction band.
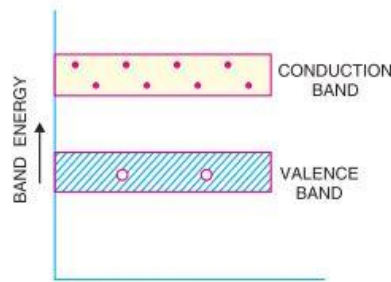
Figure 2.7 Energy band description of n-type semi-conductor [54]

The conductivity of an n-type semiconductor is mainly depends on free electrons i.e. negative charges. This type of conduction is named as n-type or electron type conductivity. It can be said that the conduction mechanism is same as in conductor (metals) like copper [54].

2.2.4 p-Type Extrinsic Semiconductor

A counteractive impact is created by the adding elements to elemental semicondustors from Group IIIA of the periodic table. Group IIIA element has trivalent substitutional impurity like gallium, aluminum and boron. When semiconductors are doped by these elements, a deficiency showed as a hole that is able bound to the impurities atom. That hole is the unconventional from the impurity atom which using the transmission of an electron from a neighboring bond as showed in Figure 2.8. In essence, the hole and the electron change locations.
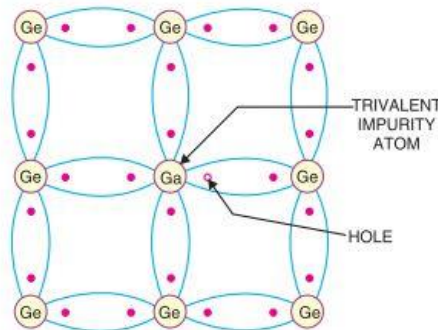
Figure 2.8 P-type extrinsic semiconductor [54]

The band model is signified the extrinsic excitationsof the semiconductors in which holes are produced. The energy level inside the band gap of extrinsic semiconductors is presented very near to the highest of the valence band shown in figure 2.9. A hole generated in the valence band using the thermal excitation of an electron from the valence band is imaginary to be into this impurity electron state. With the excitation, the hole in the valence band is generated by only one carrier; also a free electron is not generated in either the impurity level or the conduction band. This kind impurity is named as an acceptor, because it is able to accept an electron from the valence band

which leaves a hole behind. Also the energy level inside the band gap is called as an acceptor energy state due to this type of impurities. [54].
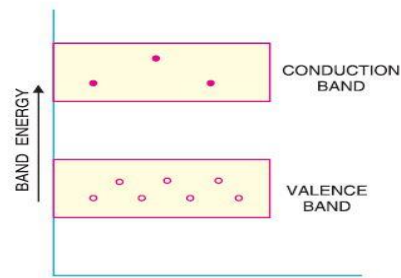
Figure 2.9 Energy band description of p-type semi-conductor [54]

2.3 Structure and Properties of Cadmium Selenide

The made-up of dual metal chalcogenide of group II–VI semiconductors in a nanocrystalline arrangement has been a quickly increasing range of study because of its significant physical and chemical properties such as non-linear optical properties, luminous properties, photoconductive properties and quantum size impact. Cadmium selenide (CdSe), one of the binary semiconductor compounds belonging to the II–IV groups of the periodic table, has bright luminescence in the evident range of optical spectra and has exposed potential usage in nanocrystalline materials. Cadmium selenide (CdSe), is an inorganic compound with the molecular weight of 191.37g/mol, mean atomic weight of 95.69 amu, mean atomic number of 41, and the enthalpy of formation equal to -136.4 kJ/mol. There are three known CdSe allotropes. The hexagonal CdSe has the wurtzite crystal structure (Figure 2.10 b) with lattice parameters at 300 K, a = 0.42977 $\pm$ 0.00010 nm and c = 0.7002 $\pm$ 0.00010 nm; the cubic allotrope, c-CdSe, possesses the sphalerite structure (Figure2.10 a) with lattice constant at 300 K of 0.64805 $\pm$ 0.00006 nm. The cubic allotrope is metastable and converts into CdSe upon heating; the transition starts at about 400 K and is complete in about 18 hours as a result of exposure to temperature close to 1000 K. The third CdSe allotrope is a high-pressure phase with rock salt structure under pressure they both convert to a denser cubic rock salt phase at a moderate pressure of 2.5 GPa and the lattice parameter of 0.554 nm. The coefficient of thermal development of CdSe at room temperature is $(2.45 \times 10^{-6}\text{l/K})$ along and $(4.40 \times 10^{-6}\text{l/K})$ across the c axis. The maximum melting point of CdSe at the pressure of 41 KPa is 1512 K. The CdSe micro hardness is between 0.9 and 1.3GPa,

depending on the crystal orientation. The band gap of Cadmium selenide differs between its different structures and the rock salt takes the smallest recording band gap of (0.6 eV at 3 GPa). Cadmium selenide single crystals crystallizes either as sphalerite (cubic, zinc blende) structure with space group *Fm3m* or as wurtzite (hexagonal) structure with space group *P63mc* and its atomic arrangement. The CdSe is a direct semiconductor with minimum energy gap at 300 K equal to 1.72 eV. The band structure of c-CdSe in most of its feature is similar to that of CdS. The electron effective mass in CdSe is 0.13 m_o, the relatively low election effective mass explains the persistent n-type conductivity in the samples of CdSe. The Hall mobility of electrons in CdSe at room temperature varies between 450 cm^2/(Vs) and 900 cm^2/(Vs) and the hole mobility between 10 cm^2/(Vs) and 50 cm^2/(Vs). CdSe has potential application in electric and photonic devices like field effect transistors, light emitting diodes, photodetectors and solar cells [57]. The Bohr radius of Cadmium selenide is about 5.6 nm. Some researchers stated that chemical deposition Cadmium selenide thin film onto the glass substrates are also cubic structure or hexagonal. The Crystal parameters of cadmium selenide for cubic structure is $a = b = c = 6.077 A°$ and the hexagonal one has $a = b = 4.299 A°$ and $= 7.010 A°$. The hexagonal structure of cell of the sphalerite is orientated in the (111) cubic direction is taken as hexagonal (001), with hexagonal axes associated to the cubic ones as $C_h = \sqrt{3}a_c$ and $a_{c} = (1/\sqrt{2})a_c$. Both formulae change basically to the packing along the ternary axis, which is a example of sphalerite fcc and wurtzite hcp in the. CdSe single crystals have a specific density of 5.816 g/cm^3, melting point of 1541 K and the micro hardness of w-CdSe is about 0.9 GPa and their thermal conductivity is 3.49 Wm^{-1} K^{-1}[57].
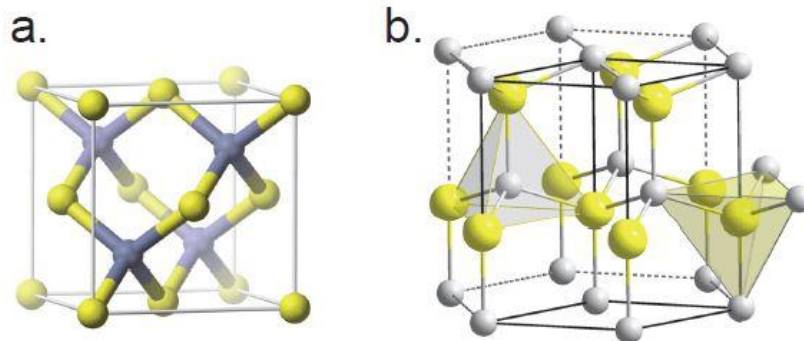
Figure 2.10 (a) Sphalerite crystal structure, (b) Hexagonal crystal structure [54]

2.3.1 Fundamental Absorption Edge

The valence to conduction band transitions or exciton transitions of electrons can be referred to as the fundamental absorption. This brings about the possibility of knowing the type of transition, energy width of the forbidden energy gap as well as significant information about the band structure of a material [55].

On the other hand, the absorption edge has to do with the discontinuity at the wavelength where the incoming photonenergy is equals to or greater than the binding energy of the particular electronic shell. The minimum energy required for the transmission of an electron of the ground state (top of the valence band) to the excited state (conduction band) that viewed in which figure is the band gap energy. Absorption of the threshold energy (band gap energy) by an electron will facilitate its transmission of the ground state to the excited state.
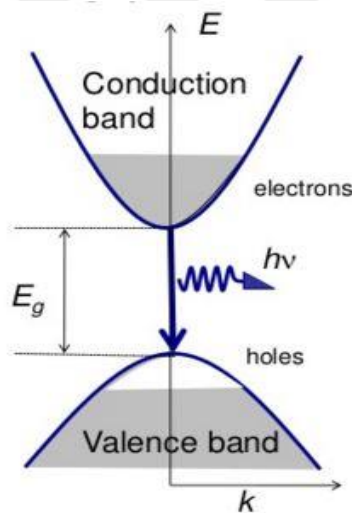
Figure 2.15 Energy band gap. Excitation mechanism of electrons to the conduction band [55].

2.4 Optical Absorption

It can be linked to a number of optical phenomena with cases of light on crystalline solid, as well as non-amorphous solid (glass). This reflection and refraction and absorption, transport include as well as. A assortment of electronic processes may share in to the phenomenon observed, but it is focused on the absorption of this work process. Basically, the electromagnetic energy in the ultraviolet-to-visible area is absorbed by

electrons of individual atoms, Causing shifts in the especially electronic process. According to Beer-Lambert's law, the absorbance can be given as:

$$A = Log\frac{I_o}{I} = \varepsilon l c = \alpha c$$

Where I_0, I, ε, l, c and α are the incident light intensity, transmitted light intensity, molar absorptivity, path length of the sample (thickness of the sample), concentration of the absorbing ions and the absorption coefficient, respectively. The plot of the absorption coefficient versus the wavelength gives the spectrum that characterizes the sample in hand. Thus, the absorbance measurement through a series of wavelengths that can help in determining the absorption characteristics of samples. To a particular wavelength of light can be choice from the light source using a monochromator. Glass sample placed across the path of this wavelength, the light transmission glass sample with less intensity because of absorption [58]. Optical property of the semiconductor is founded use the interface of electromagnetic scattering through the substance that mains to the creation of several signals as a consequence of methods like emission, reflection, absorption and scattering, show Figure 2.11. Optical description systems of these methods are used. There is extensive assortment from likely formations of the two, optical device and light sources available for optical properties of semiconductors. Previously stated, the major compensations of optical methods, associated with those that use particle accused excitement packages, it includes that the capability to analysis the samples in the air and the lack of charging in insulate material. Optical description of processes is in greatest cases, contact less and nondestructive nature, and are therefore well suitable into on-site description and procedure control, like thin-film deposition procedures.
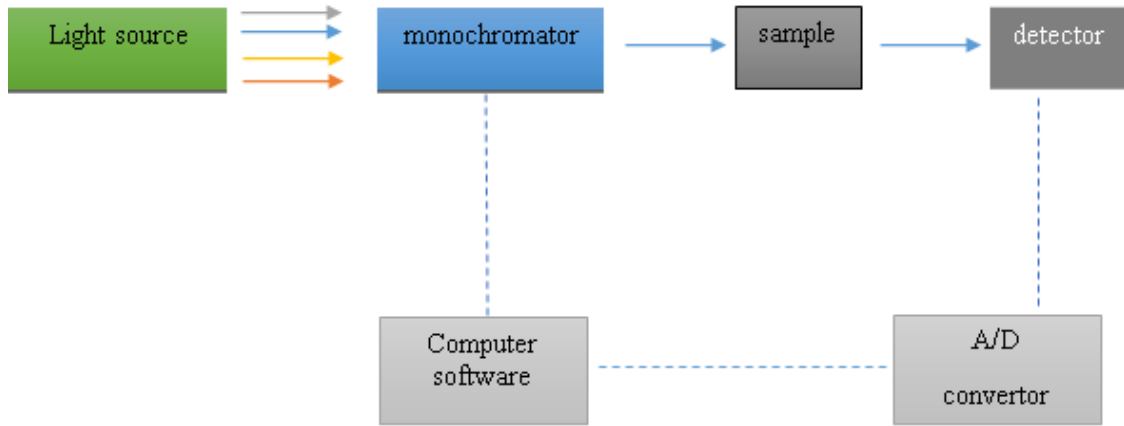
Figure 2.11 Schematic diagram of a typical UV-vis spectrometer

The major optical process for description of semiconductor involves optical microscopy, optical absorption, optical transmission, photoluminescence, the Raman spectroscopy, measurement elliptical, and coding methods.
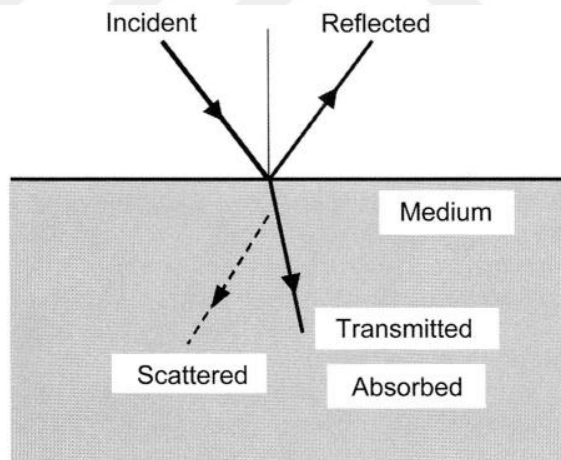
Figure 2.12 Schematic representation of various optical processes occurring as a consequence of interface of the event radiation through a medium. Scattering processes include Brillouin and Raman scattering. Some of the absorbed radiation may also be emitted leading to photoluminescence.

Generally, there are several optical absorption methods, and the total absorption coefficient α, contributes to the each other. This mechanism contains (i) free carrier absorption, (ii) absorption because of intra band transitions, (iii) absorption because of

dopants and imperfections, (v) exaction absorption and (iv) fundamental absorption process. Energy gap, smaller than the photon energies, the absorption mechanism is because of the transport of electrons of loaded valence band level to the empty conduction band level.

E_{final} ——————— ↑ ——————— $E_{initial}$

$E_{initial}$ ——————— ↓ ——————— E_{final}

Optical absorption   Optical emission
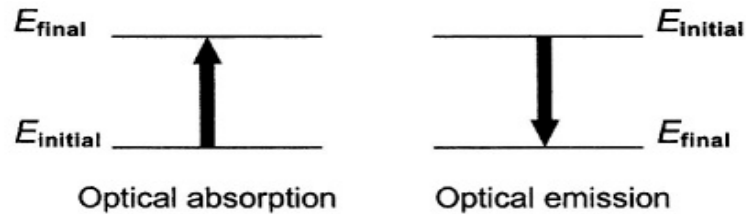
Figure 2.13 Schematic illustration of optical absorption and emission processes; the arrows indicate the electronic transition.

in energies, a little under the energy gap, the absorption mechanism is because of the excitation and transition among band states and impurity (e.g., valence band to donor and acceptor to conduction band). The transitions of the result energy bands in the process absorption continue by depress energies because free carrier absorption. Absorption mechanism is summarized farther. In a fundamental absorption process, a photon stimulates emitted energy from the photons also it has enough energy to promote the conduction band. During this process, energy and momentum is conserved. If the maximum of a valence band and minimum of conduction band was lying on same value of the wave vector K, also electrons transmitted to the conduction band directly, that semiconducting material is called as a direct gap semiconductor. If the maximum of the valance band and the minium of conduction band were not lying on the same K-value, transmissions was indirectly, then that type of material was named as an indirect gap semiconductor. Absorption in indirect gap semiconductors is comparatively weakened as associated with direct gap materials.
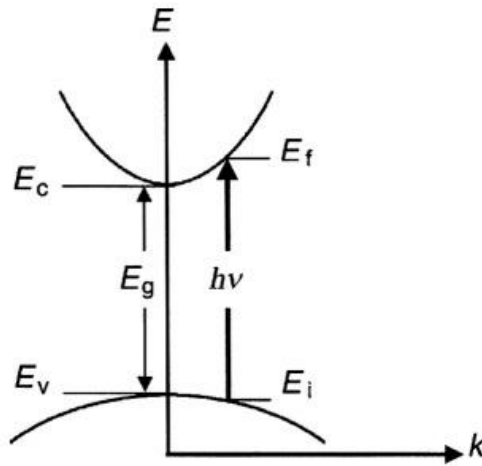
Figure 2.14 Schematic diagram of the absorption transition between direct parabolic bands.

The direct transitions among the parabolic valence band and conduction band, the absorption coefficient is

$$\alpha(h\nu) = A(h\nu - Eg)^{\frac{1}{2}}$$

where A is a constant $(A \approx 10^4)$, Eg is the band gap energy [58].

2.5 Energy Band Structure

The material be classified in the nature to conductors, semiconductors and insulators through their capability to conduct the electricity. It's a common principle that insulators do not conduct electricity, conductors conduct electricity easily and semiconductors are materials having electrical conductivity between conductors and insulators. Atomic structure of a solid material is formed by means of bands. When a solid material is formed the electrons arranged according to allowed energy level. Also the electrons do not expand and shape bands with forbidden gaps. Insulator is a material that cannot conduct electricity because its highest occupied band, the valence band was fully. Valance band is full with electrons so they cannot transfer to anywhere, then they are stable in valance band for transfer current; hence the materials are insulators. The next allowed band is the conduction band which is located overhead the valence bands in energies usually greater than 3 eV, thus it's not thermic available, and residue basically empty. The insulating material at room temperature T=300K has not enough energy to promote from the valence band to the conduction band; hence there is no conduction [60]. The difference semiconductors and insulators is a substance convention. One

29

approach is to consider semiconductors a kind from insulator through a less band gap. Contrariwise, metal is very highly conductive material. Metals were solids in which the conduction band was only partially full. Conduction band consist then of several electrons and several empty states. A big current could be maintained inside a metal then greatest of the electrons inside the conduction band may donate to the current conduction since there exist several vacancies into which the electrons may transfer below the act of driving field. Therefore, metals possess a higher electrical conductivity. The conductivity of semiconductor is more complicated than that of metals because, besides the electron scattering processes being temperature dependent as in a metal, the real number of current carrier N and their energy allocation also varies with temperatures. The resistivity of a material measured that how hard it is for a current flow. Semiconductor has a resistivity among ($10^{-4} < \rho < 10^{-8}$) Ωm.

A half-filled band are exposed on figure (2.16a). this state happens in materials containing of atoms, which contain only valence electron per atom. Greatest conducting metals counting silver, copper and gold content this stipulation. Two overlapping band is shown in figure 2.16 b. materials containing of atoms that comprise two valence electrons may still be very high conducting if the subsequent full band overlaps through an empty band. No conduction is probable for figure 2.16 d. where a fully filled band is separated of the next higher empty band by a bigger energy gap. This material performs as insulator. Lastly figure 2.16 c. shows the state in a semiconductor. The fully filled band is now near sufficient to the next very high empty band that electrons may jump the next higher band. This yields an almost full band below an almost empty band.
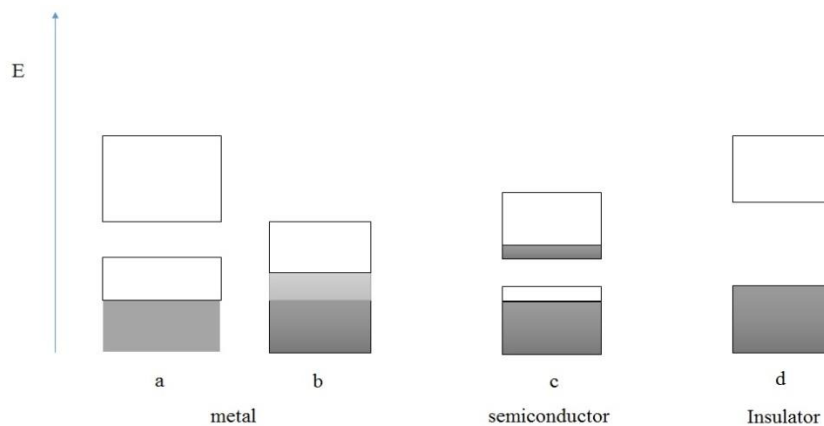
Figure 2.16 Possible energy band diagram of a crystal a) a half-filled band, b) two overlapping bands, c) an almost full separated by a small band gap from an almost empty bands and d) a full band and empty band separated by a large band gap.

2.5.1 Direct and Indirect Band gap

The band gap can be explained as the lower energy difference among the bottom of the conduction band and the top of the valence band. The top of the valence band and the bottom of the conduction band usually have not the same momentum value. The common measurable of band levels, the wave function of a single electron roving by a completely periodic lattice is expected the shape of a plane wave moving in the X-direction through propagation constant K, similarly named a wave vector. A direct band gap has the maximum value of the valence band and the minimum value of the conduction band happen at the same K value. Thus, a free electron can be created with the lowest energy conversion from the conduction band to the valence band because they do not need to any change in the momentum. Will be emitted energy and recombination across the gap in the shape of a photon of light. This is radiative recombination, as well named spontaneous emission. An indirect band gap and a direct band gap conduction is shown in Figure 2.17.
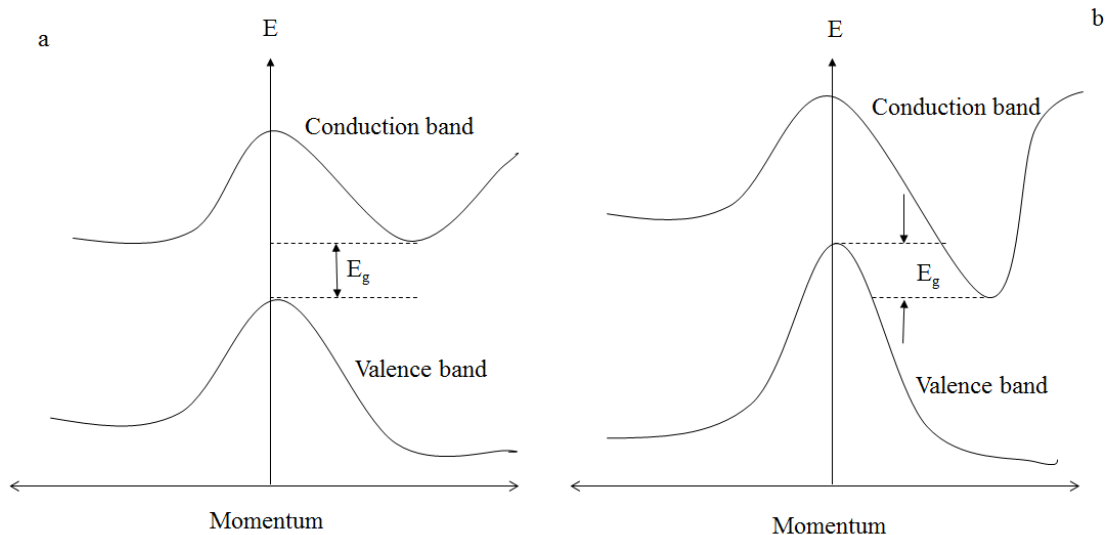
Figure 2.17 Scheme of band gap. a) direct band gap b) indirect band gap

Recombination happens with the interposition of a third body, like a crystallographic defect or phonon, which allows of preservation of momentum. This recombination

should frequently issue the band gap energy as phonon, in place of photons, and so do not emission light. In several materials with an indirect gap the maximum of the valence band is higher than the minimum of the conduction band in energy also the value of the gap is negative. This type of materials are identified as semimetals [62].

2.6 Structural analysis

2.6.1 Introduction

Structural propitiation of the main objective is to define three-dimensional arrangement of atoms in solids. In training, the main objectives is getting information about the unit cell, the lattice structures. Usually materials have some defect such as cracks, vacancies. Cracks is an example in macroscopic scale and vacancies are examples of microscopic scale. The structural properties of semiconductors can be analyzed by Scanning Electron microscopy, Energy-Dispersive X-Ray analysis in the electron microscope and X-ray diffraction techniques. All of the can be used for derive structural information, like crystalline type, microstrain, crystalline defects, phase conversions, and stresses avaible in the material [62].

2.6.2 X-ray Diffraction (XRD)

One of the stronger mechanism to the description from the structural property of semiconductor is the X-ray diffraction (XRD). The beam of collimated X-rays send to the material and scattered X-rays are detected with the suitable detector. X-ray diffraction pattern may have recorded. X-ray diffraction pattern contains of many peaks in the dispersed X-ray intensity designed as a function of 2θ angle. In X-ray diffraction, the X-rays deflected from a crystalline material can be define by using to Bragg's law that shown in the figure 2.18. Many structural properties can be idenfied by this XRD peaks such as current, strain, crystal structure, defects, crystallite sizes, orientation and crystal structure [61].
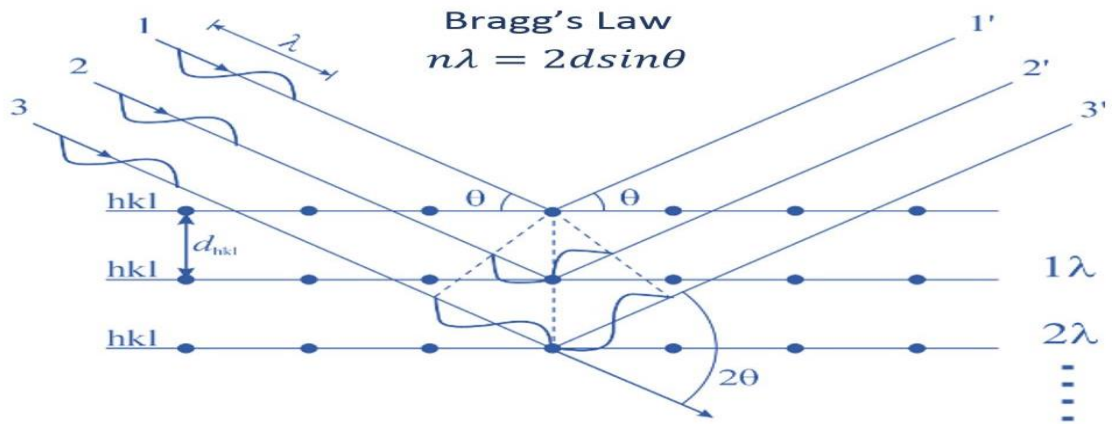
Figure 2.18 X-ray diffraction

2.6.3 Scanning Electron Microscopy (SEM)

The scanning electron microscope (SEM) is one of the widely hopeful mechanism for produce particle distribution profiles in addition to surface characteristics with the prospect to optically re-correct the data by re-assessing the particle. The mechanism grips promise for description of the size and shape of indefinite products with comparatively wide allocation profiles of the nanometer to the micron range [59]. Similarly, more frequently, SEM are prepared with energy-dispersive X-ray (EDX) detectors, which are utilized to analyzing local essential configurations in thin film. But, the likelihoods of analysis in scanning electron microscope go far beyond imaging and compositional analysis. It should be displayed imaging is divided to production utilize from secondary electrons (SE) and of backscattered electrons (BSEs), subsequent in various inverse in the images and so, provided that information on conformations, microstructures, and surface capacities. Likewise, it will be established how significant it is to combine different mechanism on identical sample locations, in order to improve the explanation of the consequences gained from applying discrete SEM mechanism. The schematic of SEM is viewed in Figure 2.19. The rule of process of scanning electron microscope involves of scanning acceptable beam of electrons transversely the sample surface [59].

In general SEM is nicely applicable to evaluate grain size, surface coarseness, porosity, particle size deliveries and material sameness. Shape and distribution of the crystallites of CdSe thin films were also studied from scanning electron microscope.
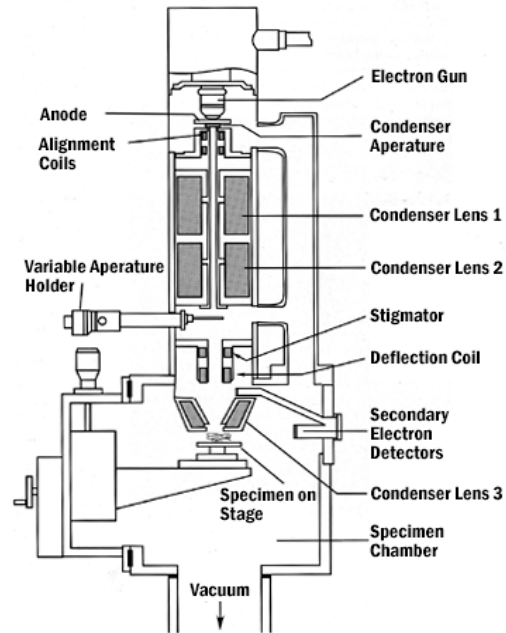
Figure 2.19 Diagram of an SEM column showing the arrangement of the magnetic lenses used to focus the beam.

2.6.4 Energy-Dispersive X-Ray analysis in the electron microscope (EDX)

EDX analysis in the SEM is, perhaps, the more public application of X-ray microanalysis. With care taken, it is imaginable to become most advantageous quantitative consequences of a widely range of materials. Unfortunately, it is also possible, especially for the novice, to misinterpret the data wildly. It is, therefore, critical that all users, not just those looking for accurate results, have a clear knowledge of the fundamentals of the technique, and the prerequisites for quality microanalysis. This contrasts, to some extent, with EDX microanalysis in the TEM. The scanning electron microscope column methods attentive investigation from electrons on the sample. The beam energy is adjustable in the range 1-30 keV or thereabouts, and the probe current is approximately in the range 10^{-8}-$10^{-11}A^0$. The probe diameter is typically in the range 1-10 nm (of course, all the values quoted here are generalizations). The scan may also be stopped, and the beam steered to a specific point on the sample surface, so that the emitted radiation from that point may be analyzed in detail. Production of X-rays can take place at any depth where the electron beam has enough energy to ionize the atoms. The probability of X-ray production will vary with depth, in a way that will vary from element to element. The details of these processes will form the subject of discussion of

34

a large portion of this chapter, but it is clear that the volume from which the X-rays originate is substantially the whole interaction volume of the electron beam. While the X-rays can be absorbed as they pass through the material of the sample, they have, in general, a much longer path than electrons, and so have a good probability of leaving the sample and reaching the detector. Thus, the spatial resolution of the X-ray signal is variable, and is frequently of the order of a micron or more. We will conclude this introduction by making a few remarks about the electron microprobe. In principle, the electron microprobe is simply an SEM, on which has been mounted one (or, more usually, several) crystal X-ray spectrometers. The crystal spectrometers detect the X-rays with far higher energy resolution than does the EDX detector. While the resulting improved peak-to-background certainly contributes to the improved sensitivity of the microprobe, it is not the main factor the maximum count rate of the EDX detector is limited to a few thousand counts per second. The crystal spectrometers, in contrast, can count much faster, thus providing better statistics in the X-ray analysis. However, this count rate can only be achieved if enough X-rays are generated in the sample. The electron beam currents typical of SEM imaging are not adequate to generate these count rates. Therefore, the electron column of the microprobe is designed to produce electron probes with far more current, and correspondingly larger probe sizes, than the SEM. It is also necessary that the probe current be extremely stable over the time of the measurement (because the data acquisition in the microprobe is serial in nature, and the conditions must remain the same over the time of the experiment). This requirement is introducing some design constraints into the system [61].

CHAPTER 3

EXPERIMENTAL STUDIES

3.1 Introduction

Spray pyrolysis method is a multilateral and conventional way to deposited metal oxide film. It is very useful for wide area deposition of the film materials for different manufacturing applications. Spray pyrolysis satify to control the film quality easily. The morphology and characteristics of the films are hugely dependent on the deposition method. A lot of significant structure is that the surface temperature of the substrate temperature. Films are broken when the temperatures are very low. In betwixt, intensive soft films can get. The deposition temperature is very impacts the crystallization, consistency and another physical property of the deposition film. Precursor solution is the other important spray stricture affecting the morphological and characteristics of the deposition film. Moreover, the characteristics and the film morphological may alteration dramatically through the use of the different additives in the solution of precursors.

The group II–VI of compound semiconductors entice extra attending because of their wide range of applications in the many fields such as photo-detectors in optoelectronics applications, [63,64]. Gas sensors, photoconductive cells, thin film transistors, optical wave guides, light emitting diodes (LEDs), and solar cells [65]. CdSe is a well-known compound semiconductor of this group. Cadmium selenide have a direct band gap (1.74 eV) at room temperature, n-type conductivity and high absorption coefficient in the visible range [66]. CdSe is the greatest broadly studied semiconductor because of its photoconductive properties. They used as a photoanode in photoelectrochemical cells (PECs) and photoconductive cells. They have high energy-conversion efficiency about 16.7% [67]. Cadmium selenide films have quantum confinement impact. It is defined by

the investigated separate electronic energy levels in the microscopic structure of nanocrystalline. Cadmium selenide films have greater carrier mobility than silicon films. The low cost deposition methods and high quality of thin films is very preferred for optoelectronic device applications [15].

3.2 The Thin Film Production Methods: Spray Pyrolysis Method

Spray pyrolysis enclose spraying a fine mist of tiny droplets consisted of the reactants on the spicy substrate similarly, the catchy technique for growing semiconducting films because of it is easy, and it is able to deposit uniform layers are commonly in a perfect mixture of the material to form an alloy. The deposition method produces to control too many spray parameters like, solution spray rate, deposition time and the substrate temperature.

Spray pyrolysis is an appropriate mixture to spray at a hot substrate, wherever the element interacts to compose a chemical solution. Chemical reagents are chosen because of the other produce of the required combine are changeful in the degree of deposition temperature.

Spray pyrolysis method easily consist of spraying a soft atomized resolution at a convenient substrate. It is expected to fulfill the following conditions are met where the chemicals contained in the spray solution:

a) In thrombolysis, the chemicals in resolution shape must be provide species/complexes will be submitting chemical reaction thermic excited to produce the required thin film material.

b) It should be the rest of the alternatives, including the unsteady liquid transport temperature of the substrate. The substrate has large effect on the deposition operation and substrate warming and temperature control in the process of average spraying, the geometry of the spray nozzle is affected the volume of the sprayed particles and the spray patterns.

After atomization, the transport gas stream drops minutes on a heated substrate with the approximation of drops from it, at ideal situation, and is anticipated to evaporate completely, resulting in the deposition of non-volatile components of the dissolvent. yet,

the difference in the droplet volume to the emergence of a number of different depositional processes, depending on the thermal conduct of droplets sized differently. In this study, it is a device which is used expansion of film founded on samples spray method has been designed and advanced in our laboratory. A graphic diagram of an empirical apparatus used for spray pyrolysis is seen in figure 3.1. This system consists of a spraying system, heater, temperature control system, and timer. The system is enclosed by a glass chamber.

Spraying system: that is used for produce the bubbles on the spraying solution. The bubbles can be in various size rely on the geometry of the nozzle, as known in figure 3.1. In this study, air used to transport gas and the influx rate of spraying solution is controlled by air.

Heater: That is used for temperature the substrate. Is contain of a steel plate with a resistance coil lying under it. The powder of the heater is 2500 watts and it operates at 220 volts and 50 Hz (AC).

Temperature control system: a thermostat is used to save the substrate at desired temperatures. One of the most important factors that play a necessary role to produce high quality film samples is maintained the substrate at desired temperature. It is controlled by the temperature of the substrate during the accuracy of ± 5 ^{o}C by thermostat system.

Glass chamber: Spraying system is put heaters in a glass chamber and gas is nitrogen passed out of a thin layer during the produce of the thin film.
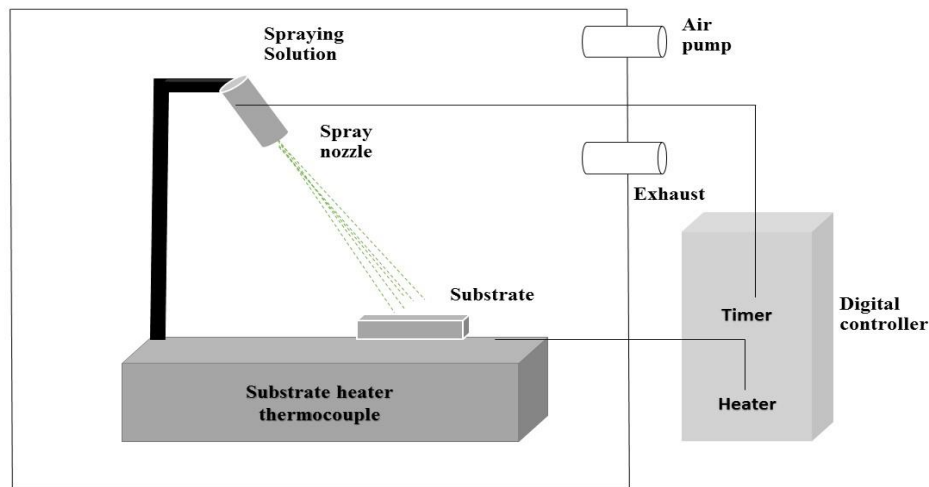
Figure 3.1 Schematic diagram of the spray pyrolysis system

3.3 Substrate Preparation

Cleaning and preparation of substrates is a fundamental for success in the thin film production. Physical properties of the substrate which is deposited thin films, plays a necessary role in the produce a good quality thin samples. The film properties are very hard relying on the crystal structure of substrate. Condensation rate and cohesion of the deposit are critically relying of conditions on the surface. Even a thin layer of grease can have such a total impact at the molecular scale to completely change the layer properties. glass, ceramic and mica is a non-crystalline material can be placed at the crystalline films. Glass is used as the substrate due to its cheapness compared with other kind of substrate. The preparation of the glass substrate is as follows. Firstly, the glass substrate is cut in the area (0.5×1.0 cm^2) in size. It must be followed to prepare the following cleaning and surface conditions directly before to application. Cleaning process with a cloth solvent can be able to clear any grease, oil or drift. It is cleaning process substrate in four steps, as seen in Figure 3.2.
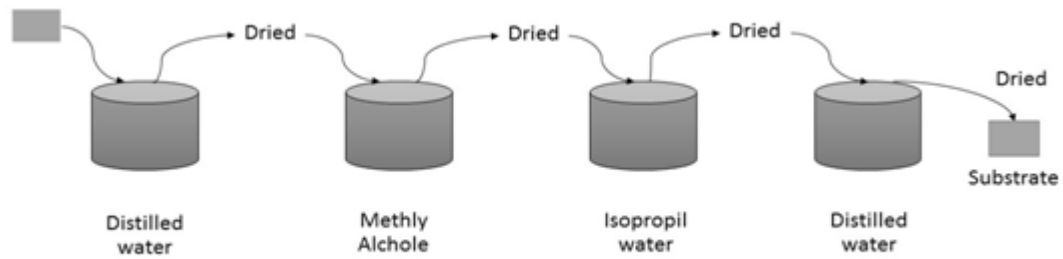
Figure 3.2 The cleaning process of the glass substrate.

3.3.1 Cleaning Process of the Glass Substrate

The cleaning process to security the substrate is totally clean and contaminant free included four joint steps as follows:

- At the beginning the glass substrate is immersed at the distilled water to clean the powder on its surface for 15 minutes. And then taken out of distilled water, and dried.

- Substrate taken from the first cup dried, and immersed in methyl alcohol and leave for 15 minutes to clear the oil on the surface of the substrate material, and then taken out of the liquid and air-dried.

- Dried substrate immersed in the third cup filled with isopropyl alcohol was dealing with her again for 15 minutes to get a smooth surface.

- Finally, it is treated with the substrate with distilled water as the first step to clean up all of the remaining residue on the surface of the substrate through other processes.

3.4 Development of Thin Films by Spray Pyrolysis Method

In this study, it was obtained cadmium selenide semiconductor (CdSe) by spray pyrolysis under various deposition conditions.

3.4.1 Development of CdSe Thin Films by Spray Pyrolysis Method

CdSe thin films are deposition on so clean glass substrate nearly (0.5 cm^2) of geometric area at substrate temperature were protected to (225, 250, 275 300, 350, 400 °C) by using controller electronic temperature with a precision of ± 5 °C, respectively by use spray pyrolysis method. The films are prepared by the aqueous solutions containing cadmium

chloride (CdCl$_2$ Merch, purity 98%) and selenium oxide (SeO$_2$) Merch, purity 98%). The solution was prepared by spray for the produce of cadmium selenide thin-film, it will have done some steps to produce the chemical solution, the molar ratio of Cd/Se closefisted in to three step. Firstly, the first solution is prepared with 0.502 gm CdCl$_2$, 50 ml distilled water H$_2$O and mixed stirred 10 minute at 600 rpm secondly 0.3 gm SeO$_2$ and 50 ml distilled water mixed stirred for10 minutes at 600 rpm and finally both solution is mixed together in a big baker then stirred for 30 minutes at 600 rpm for preparing spraying chemical solution. After producing the solution CdSe, next step is boron doping to the chemical solution. The pressed air by the air pump as transport gas is satisfies the atomization of the chemical solution into a spray of accurate droplets. The spray flow rate was modified to nearly 0.5 ml. minute, the height of the nozzle was fixed to 20 cm form the substrate surface placed on the heater. During the spray operation, the temperature is increased by the electrical heater, because of the substrate must be heated. During the experimental studied the different temperature is used as 225°C, 250°C, 275°C, 300°C, 325°C and 350°C. When the solution droplets reach the heated glass substrate surface, the chemical reactions are next happened. The films produced at 275^{0}C has best properties which is mentioned later at results and discussions' chapter, so doping process is applied for this temperature. Firstly, the boron is doped CdSe at (T=225°C): (100 ml of the solution (0.1 M CdCl$_2$, 0.1 M SeO$_2$, 0.01 M H$_3$BO$_3$)), at (T=275°C): (100 ml of the solution 0.1 M CdCl$_2$, 0.1 M SeO$_2$, 0.05 M H$_3$BO$_3$), at (T=275°C): (100 ml of the solution 0.1M CdCl$_2$, 0.1 M SeO$_2$, 0.025 M H$_3$BO$_3$), at (T=275°C): (100 ml of the solution 0.1 M CdCl$_2$, 0.1 M SeO$_2$, 0.015 M H$_3$BO$_3$) at (T=275°C): (0.1 M CdCl$_2$, 0.1 M SeO$_2$, 0.02 M H$_3$BO$_3$), at (T=275°C) (0.1 M CdCl$_2$, 0.1 M SeO$_2$, 0.025 M H$_3$BO$_3$)

$$CdCl_2 + SeO_2 + H_2O \longrightarrow CdSe + Cl_2O_3 + H_2$$
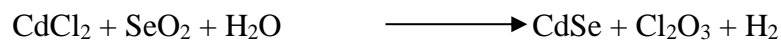
As seen from reaction, CdSe thin film is formative on the substrate surface while the Cl$_2$O$_3$ and gas disuse the system.

Figure 3.3 High sensible electronic balance

3.5 Measurements Techniques

The X-ray diffraction (XRD) and SEM analysis are the two technique that use to found the structure characteristic of the deposited films. The optical characteristic of the film was investigated from optical absorption coefficient and transmittance spectra data using double beam visible spectrophotometer. Using this data, identify the band gap energies of the deposited films.

3.5.1 The Structure Properties Measurements

X-ray diffraction provides to discovery the geometry or molecular shape by X-rays. XRD method is dependent of the flexible scattering of X-rays from structure that own for far-reaching. The structural properties of thin film can be defined by X-ray diffraction. XRD patterns utilized to the characteristics of the structure of crystals and preferred orientation of the thin-film anchored substrate. To calculation the thickness and properties of the structure of crystal and tension in the thin films, utilized the high resolution of the X-ray diffraction. X-ray measurements were conducted by X-ray diffraction (XRD) mechanism on Braker AXS D5005 diffractometer (monochromic Cukα radiation, λ=1.54056A). The XRD patterns were recorded in 2θ interval from 20°

up to 35° with the step 0.05° the peaks (2θ) of the XRD patterns of the film samples were specific by using Bragg diffraction law equation as described below. The Bragg's equation confirms a relation among the diffraction experiment and the structure parameters. The measured rate is the Bragg's angle θ and the structural parameter is the lattice spacing d_{hkl}.

$$n\lambda = 2dsin\theta$$
(3.1)

The planes are known by their (hkl) values and the d_{hkl} inter planar spacing. The geometric function of the shape and size of a unit cell are represented by the value d_{hkl}. The relation among d_{hkl} and the real unit cell is commonly stated in a various form for every crystal system.

This equation represented the lattice constant 'a' for the cubic structure;

$$a^2 = \frac{\lambda^2(h^2+k^2+l^2)}{4sin^2\theta}$$
(3.2)

Where λ is the wavelength of the X-ray, θ is the diffraction spectra (Bragg's angle), The line profiles were measured with the aid of point cutting utilizing fix interval 20s and 2θ increment of 0.02°. Form the XRD profiles, the inter-planer spacing d_{hkl} was measured for (hkl) plane using the Bragg's relationship [68].

$$d_{hkl} = \frac{n\lambda}{2sin\theta}$$
(3.3)

where θ is the Bragg's angle, d is the lattice spacing, λ is the wavelength of the X-ray used, and n is the order number. The factor d is linked to the (hkl) indicates of the planes and the distance of the unit cell. The crystallite size (D) of the films was measured from the Debye Scherer's formula from the full-width at half-maximum (FWHM) β of peak expressed in radians [69].

$$D = \frac{0.94\lambda}{\beta cos\theta}$$
(3.4)

Where β is the (FWHM) measurement from the (dkl) plane. The value of strain (ε) calculated by the equation.

$$\varepsilon = \frac{\beta \cos\theta}{4}$$

(3.5)

For the cubic geometry, the lattice parameter 'a' can be determined from the equation as shown:

$$\frac{1}{d^2} = \frac{h^2 + k^2 + l^2}{a^2}$$

(3.6)

Where h, k, l represents the lattice planes.

3.5.2 The Optical Properties Measurements

A significant technique used for limitation of the band gap energy of a semiconductor is the absorption of accident photons via material. To calculation the optical absorption studies of the spray pyrolysis on glass substrate thin films, by carried out in the wavelength range about 300 nm to 900 nm use a UV/VIS spectrophotometer. The study of the absorption of a large plurality of elements on at least part of the spectrum of the X-ray. The norm is simple to determine the absorption coefficient. Average diluted between the source and the detector, and the reduction in intensity is measured. It will be appreciated that this decrease in density may be caused either by photon absorption within a matter of interference or scattering of the beam collimated. Determine the values of the energy gap of the samples, it is essential for found the value of the absorption coefficient of the identical samples of various wavelengths of the photons. For this aim, a Jasco 7800 model spectrometer was used for transportation and absorption measurements. The absorption coefficient of sample identical to different wavelengths may be founded from the following equation:

$$\frac{I}{I_o}(transmission) = e^{-\alpha t}$$

(3.7)

When t represented the thickness of the film sample $T = I/I_o$ is the transmittance (I_o is the incident of light intensity and I is the transmitted of light intensity).

By using α values, band gap of the film sample can be calculated by means of the following equation:

$$\alpha = \frac{A}{h\nu}(h\nu - \text{Eg})\tfrac{1}{2}$$

$$(3.8)$$

Where h is the planck constant, $\nu = c/\lambda$, c is the speed of light and λ is the wavelength of light, E_g denotes the optical band gap of the film, A is a characteristic parameter (independent of photon energy), $h\nu$ is the photon energy.

3.5.3 The SEM Analysis

The SEM apparatus has much applications across different manufacture sector. Images of very high magnification along with a local chemical information enables a means to resolve many common industrial issues like molecules and materials to identify metallurgical imbalances and problems analysis. (SEM) is a device that usages electrons in place of light to from a picture. Electron microscopes have been developed because of the limit of the light microscope, which are limited by the physics of light. There are many advantages to using SEM rather than an optical microscope, the cross-section out of a focus on high-energy beam of electrons on the surface of the sample and individual discovering of the interaction of electrons incident with the sample surface. One kind of control change in a SEM and can comprise secondary electrons, properties X-rays, and back scattered electrons. In SEM, there are another signals interaction within the sample near surface, not only from offending mainly on the sample. SEM is able to create the high-resolution images of a sample surface in its fundamental utilize mode, secondary electron microscopy imaging. This is the way in which this image is created, SEM images possess a big depth of field produce features a three-dimensional manifestation advantageous for conception the structure of the sample surface. This is a large depth of field, a wide range of enlargement in and put the most familiar imaging samples in SEM.

CHAPTER 4

RESULTS and DISCUSSION

4.1 Experimental procedure for the growth of CdSe films

In this section of the study, our aim was to obtain the optimum experimental conditions for the best quality of CdSe films. Spray pyrolysis is a method which include a spraying system with a fine mist of small droplets incorporating reactants onto hot substrate. When the droplets reachs the hot substrate surface then they start to evaporate. Also the condensation of solution and thermal decomposition of volatile by products results the film formation. In this study, CdSe films were developed on highly cleaned glass substrates at which the substrate temperature ranged between $225^{\circ}C$ and $300^{\circ}C$ and an aqueous solution was sprayed in air atmosphere. The geometric area of the films is about 0.5 cm^2. The temperature was controlled within ± 5 $^{\circ}C$ through a chromel-alumel thermocouple by means of a sensor for the temperature controller.

Firstly the substrate cleaning process was done by ultrasonically cleaning in acetone solution or then rinsing in de-ionized water. The spray solutions are comprised of $CdCl_2$ (Merck, $\geq 99\%$) and SeO_2 (Merck, $\geq 99\%$) in the deionized water. The spray flow rate was setted to about 0.2 mL/min and the distance between the nozzle (head of the sprayed source) and the substrate was held at 35 cm during for all experiments. Deionized water was used as a solvent. The molar ratio of the Cadmium and Selenium source of Cd:Se=1:1 was used. The spraying solutions were sprayed onto the hot substrate at about $275^{\circ}C$ temperature. During the deposition of films, the following chemical reaction occurs,

$$CdCl_2 + SeO_2 + H_2O \text{ ----------- } CdSe + 2HCl + \frac{3}{2}O_2(gas)$$
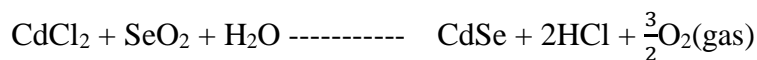
As seen from this reaction, CdSe thin film is formed on the glass substrate surface, the other chemicals HCl and O_2 release as gas.

4.2 Surface Morphological and Compositional Analysis of CdSe Film

The morphological properties of spray deposited CdSe films were investigated by using SEM technique and it was concluded that the substance having growth of good CdSe film quality at which substrate temperature. SEM analysis method is the unique, best, convenient and versatile method to analyze morphological properties of film and give imformation about grain size. Figure 4.1 shows the surface morphologies of the sprayed films as a function of the substrate temperature. It is clear that all grain properties which grain size and grain boundaires change considerably with the substrate temperature of the films. At the substrate temperature between 225°C and 300 °C, the film appears to be more uniform, smooth, and less porous with an amorphous-like structure. At the 225 °C substrate temperature, this amorphous-like matrix begins to show the fine features representative of polycrystalline films (Figure 4.1a). At the 250 °C substrate temperature, the amorphous-like matrix begins to show producing of small crystallites on the film surface (Figure 4.1b). These latter crystallites starts to show an extending on the film surface and also the best crystallinity properties was showed on the substrate surface at a deposition temperature 275 °C (Figure 4.1c).

The last one, (Figure 4.1d) is not also a good crystallinity example for filming. As a result, it is attributed that the good quality of CdSe film was grown at 275°C substrate temperature onto the high cleaned glass substrate. (Figure 4.1c) shows the SEM images of CdSe film produced at substrate temperature of 275 °C. From this SEM image, it is noticed that the sprayed CdSe film is homogenity, smooth. There was no crack on the surface area of the sprayed films because the surface morphology covering whole film area is very dense. The distributions of small sized grains were uniformly. The films have a smooth homogenous area. The grains were homogen and small. The grain boundaries were well-defined. The observed average grain size was 25 nm. The size of grain is in inconsistent for both analysis methods; XRD and SEM. The cluster types of structures were formed by composition of two or more grains coming together. The formation of the semi-conductive layers, the nucleation and epitaxial effect was defined by morphological properties. In addition, the substrate temperature affects the characteristic properties like the grain size, band gap and porosity etc.

It is shown that in the SEM micrograph, the porosity of the sprayed CdSe film was increased at the substrate temperature 275℃. Therefore, it is considered that the films deposited at 275℃ are preferable for using the photovoltaic device application.
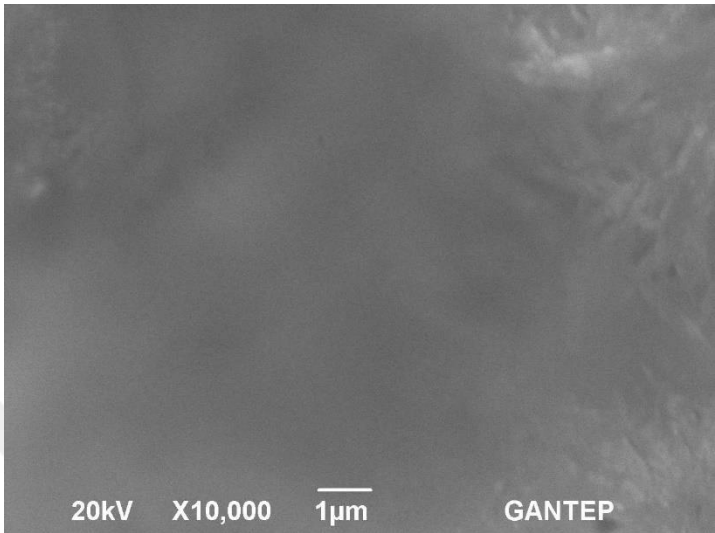
Figure 4.1(a) SEM photography of CdSe film for T=225 ℃
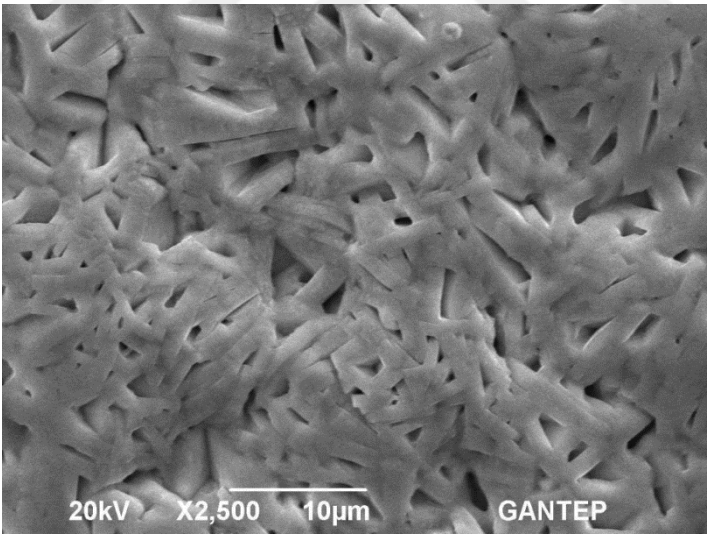
Figure 4.1(b) SEM photography of CdSe film for T=250 ℃
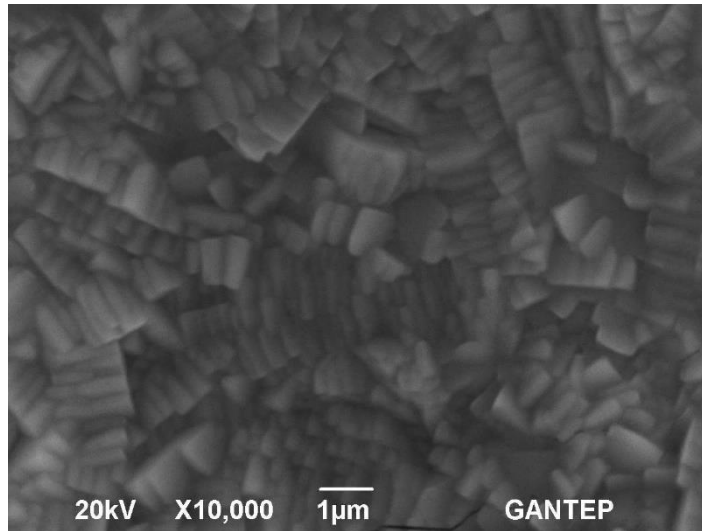
Figure 4.1(c) SEM photography of CdSe film for T=275 ℃
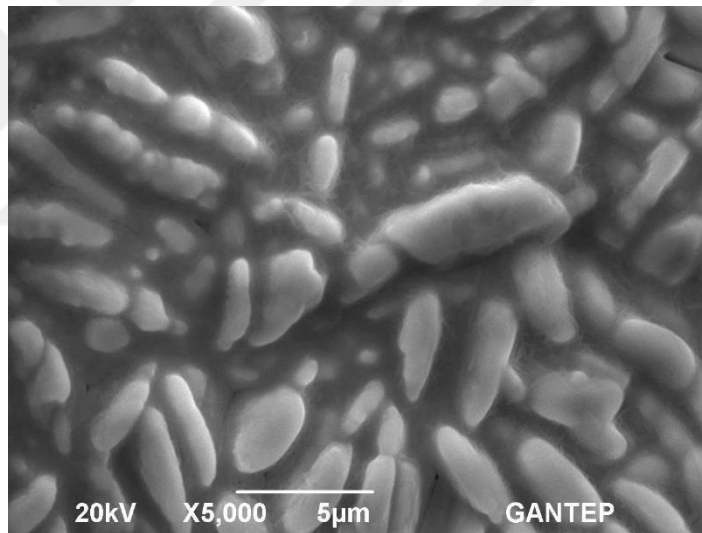
Figure 4.1(d) SEM photography of CdSe film for T=300 ℃

Energy Dispersive X-ray Analysis (EDAX) is one of the most common technique used to define the chemical composition of unknown material. According to this technique the peaks in EDAX Spectrum is identified and each peak is unique for an atom that corresponds to a single element. The chemical compositions of films also presence of Cd and Se concentrations has been determined by EDAX spectra and the results are tabulated in Table 4.1. The results in Table 4.1 have showed that the higher concentration of Cd and Se showed good stoichiometric composition.

Figure 4.2(a-d) shows us to the SEM images of the CdSe films deposited at T=275 °C substrate temperature according to the different boron concentrations of spray solution. Figure 4.2 gives the results that confirm a hypothesis to define the growth mechanism. During deposition very small fine droplets vaporize onto hot substrate. The condensation starts to form as microcrystallites with small various dimensions onto the surface of the sprayed film. It is concluded that the grain size increases when the boron concentration increases up to 0.01 M. The crystallinity of the film increases enormously with boron concentration and it is evidenced from the surface morphology study. The crystallites with large grain size are formed on smooth surface. Also, from the micrographs, it is seen the distribution of spherical grains over total coverage of the substrate is uniform. They have a homogenity and well-grained morphological properties.

The increase in grain density favours concretion between individual grains during lateral growth and an increase of the compactness of the depositions shows itself after addition of B in the solution,

Table 4.1 Compositional analysis for Cd and Se of spray deposited CdSe thin films at different substrate temperatures.

$T_{subsrate}$ (°C)	Cd (wt.%)	Se (wt.%)	Cd/Se
225	54.009	45.215	1.19
250	52.725	47.704	1.10
275	51.524	49.282	1.045
300	53.946	46.650	1.15

As seen in Table 4.1, the substrate temperature is playing an important role for the growth of the CdSe film. The molar ratio of Cd/Se has been changed during the deposition process under the influence of substrate temperature. This changing shows us also the best crystallization on the substrate at around 275 °C. The result indicates that the other important properties of the samples will be changed according to the growth substrate temperature. After deciding the best temperature for the growth of the CdSe-film on the surface glass substrate by using spraying-pyrolysis method, some structural properties were extensively investigated with XRD and SEM.
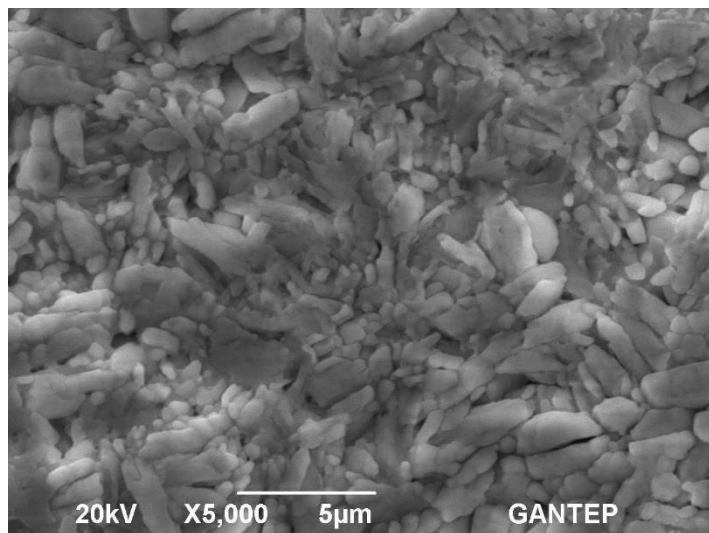
Figure 4.2(a) SEM photography of Boron (0.0025M H_3BO_3) doped CdSe film at T=275 ^{o}C substrate temperature.
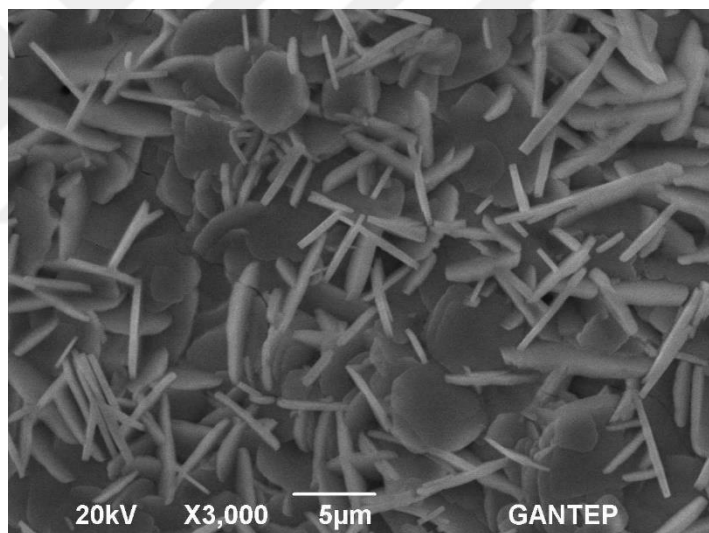
Figure 4.2(b) SEM photography of Boron (0.015M H_3BO_3) doped CdSe film at T=275 ^{o}C substrate temperature.
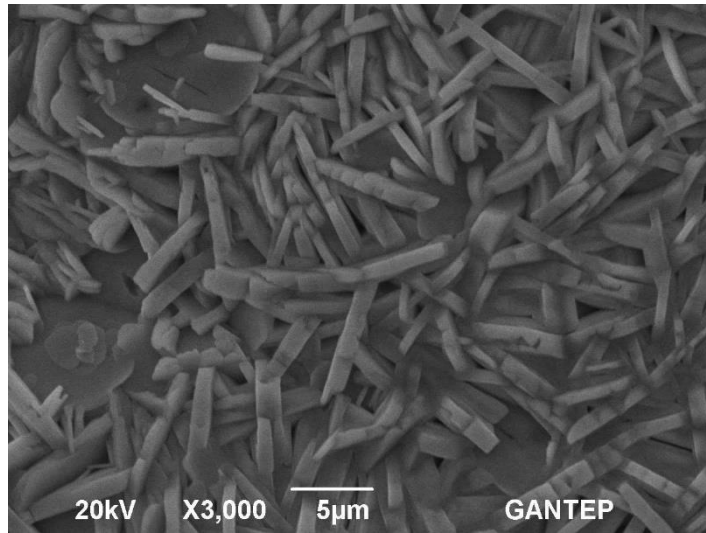
Figure 4.2(c) SEM photography of Boron (0.01M H_3BO_3) doped CdSe film at T=275 °C substrate temperature.
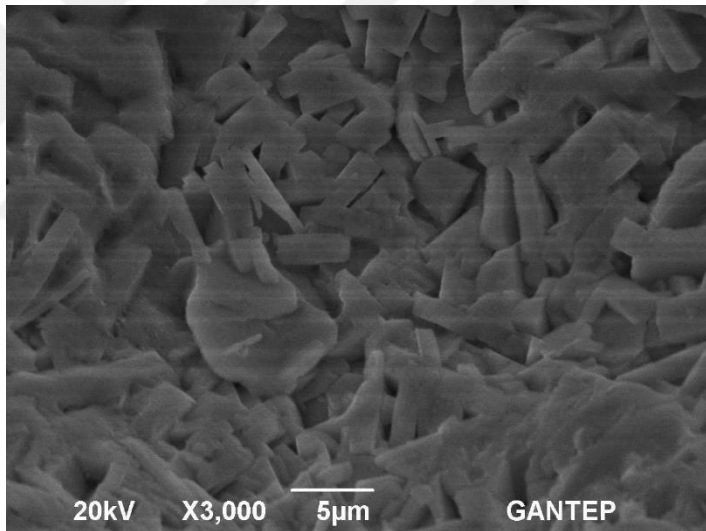
Figure 4.2(d) SEM photography of Boron (0.05M H_3BO_3) doped CdSe film at T=275 °C substrate temperature

4.3 Structural Studies of CdSe Films
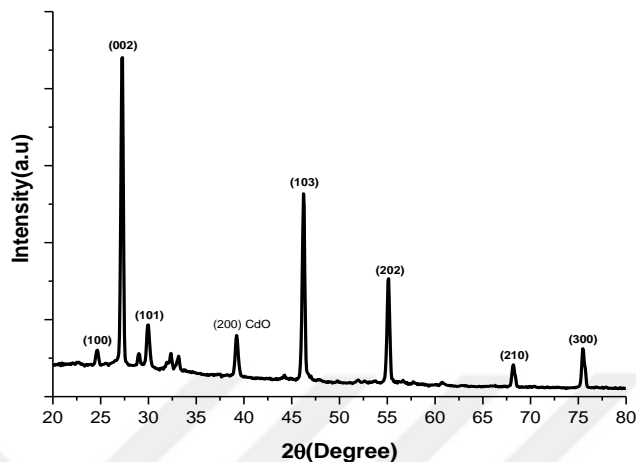
Figure 4.3 A typical XRD pattern of sprayed CdSe film at 275 °C substrate temperature.

      The crystalline structural properties of CdSe films were studied by X-ray diffraction with Cu-Kα radiation (1.5406 °A). The value of 2θ angle was varying from 20° to 80°. Figure 4.3 shows typical X-ray diffraction pattern of sprayed CdSe film deposited at 275 °C. The polycrystalline structure of the films of CdSe produced by spray pyrolysis method is revealed by the X-ray diffraction patterns. In general, CdSe shows two different crystal structures, which were cubic wurtzite and hexagonal zinc blende. A study has been reported about the CdSe films deposited by chemically deposited CdSe films showed cubic, hexagonal or mixed (cubic + hexagonal) crystal structures depending on the preparation conditions [70, 71]. However, it is noted that the undesirable cadmium oxide (CdO) phase, characterized by (200) line is present in the films [72]. The Cd oxidates during high temperature deposition, the evidence of this oxidation can be said the presence of CdO assigned. The amounts of cadmium ions are unsteady in aqueous solution and chemical balance is fastly created in solutions because of this CdO can be formed during the film deposition. Therefore the saturation of the solution due to the amount of CdO is setted instantly after the incorparating of the reagents, so the deposition of CdO is started at the first phase of the procedure. The formation of CdSe phase which desired is concluded from X-ray diffraction patterns. The XRD pattern shows several peaks at 2θ values about of 25°, 27°, 30°, 38°, 46°, 55°,

53

68° and 76° which may be assigned to the diffraction lines produced by the (100), (002), (101), (200)$_{CdO}$, (103), (202), (210) and (300) planes of hexagonal (wurtzite) structure of CdSe, respectively [70,73]. The appearance predominated peaks of the (002), (103) and (202) reflection planes at diffraction angles $2\theta = 27°$, 46° and 55° is an indication of the hexagonal (wurtzite) structure of CdSe film [74]. The appearance of many peaks in the XRD pattern is an indication of polycrystalline nature of the CdSe film. Therefore, considering our future goal of the growth of CdSe film the better deposition temperature of glass substrate is 275 °C.

4.4 The growth of Boron doped CdSe films onto the glass substrate at 275 °C.
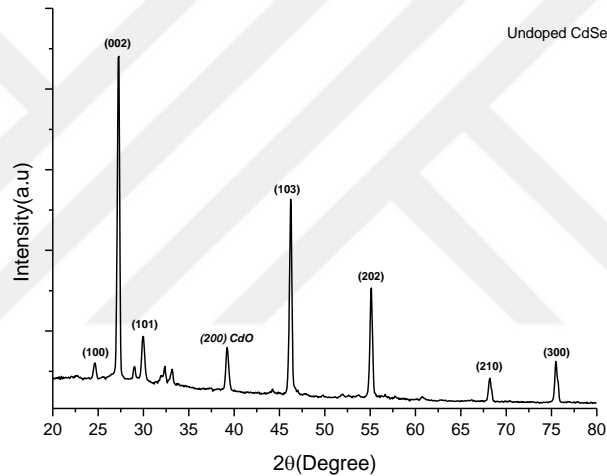
Figure 4.4 (a) A typical XRD pattern of sprayed undoped CdSe film at 275 °C substrate temperature.
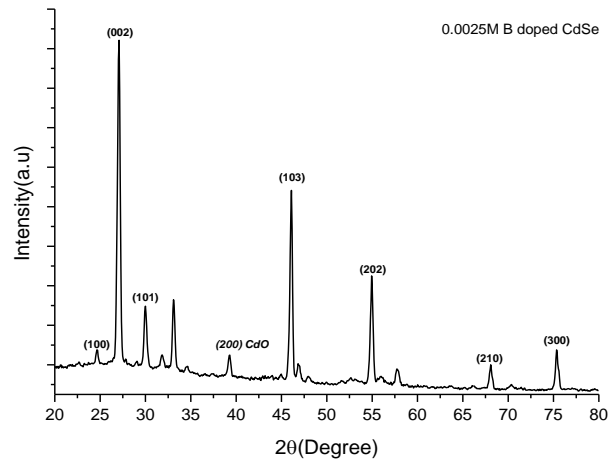
Figure 4.4 (b) A typical XRD pattern of sprayed boron doped (0.0025 M) CdSe film at 275 ℃ substrate temperature.
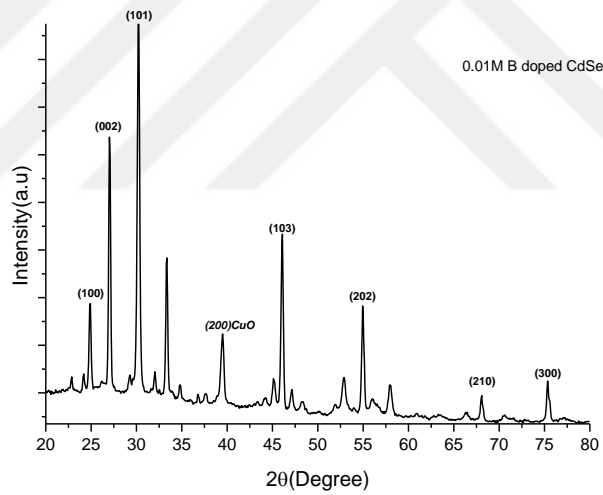
Figure 4.4 (c) A typical XRD pattern of sprayed boron doped (0.01 M) CdSe film at 275 ℃ substrate temperature.
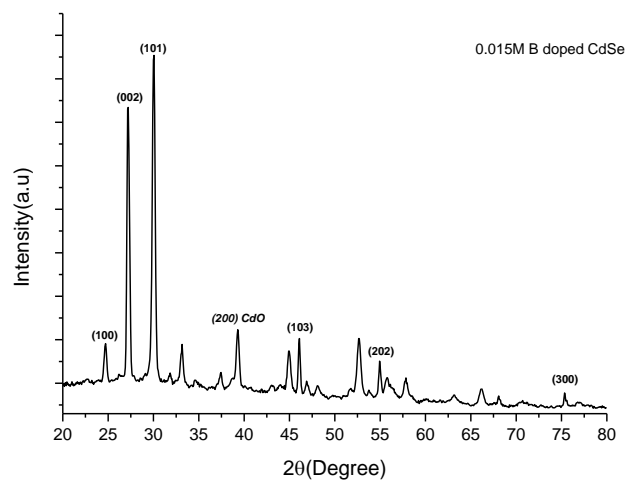
Figure 4.4 (d) A typical XRD pattern of sprayed boron doped (0.015 M) CdSe film at 275 ºC substrate temperature.
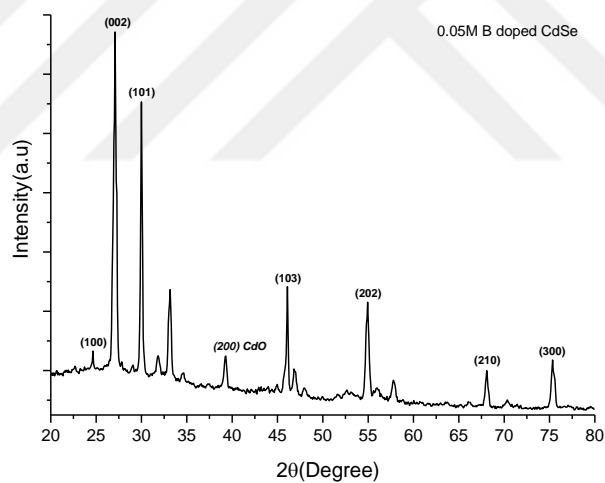
Figure 4.4 (e) A typical XRD pattern of sprayed boron doped (0.05 M) CdSe film at 275 ºC substrate temperature.

Table 4.2 XRD pattern results of the undoped and boron doped CdSe films.

Sample	2θ	Miller Index	Lattice constant a(A⁰)	Grain Size d(A⁰)	Dislocation density ε(x10⁻³)	Microstrain ρ(x10⁹)/cm³
Undoped CdSe	27.22	(002)	5.349	2.492	1.6863	6.7163
	29.92	(101)	5.412	2.501	1.6314	6.8119
	46.23	(103)	5.301	2.493	1.6301	6.8319
	55.07	(202)	5.378	2.462	1.6118	6.6835
0.0025M B doped CdSe	27.02	(002)	5.392	2.421	1.7198	6.8869
	30.19	(101)	5.426	2.563	1.5812	6.7829
	46.09	(103)	5.338	2.490	1.6801	6.8519
	54.94	(202)	5.404	2.468	1.7542	6.7736
0.01M B doped CdSe	27.15	(002)	5.402	2.393	1.8317	6.9163
	30.05	(101)	5.410	2.864	1.4769	6.7365
	46.12	(103)	5.303	2.385	1.7309	6.8819
	54.98	(202)	5.383	2.358	1.7732	6.8533
0.015 M B doped CdSe	27.08	(002)	5.382	2.327	1.8493	6.9203
	29.98	(101)	5.394	2.598	1.6012	6.7824
	46.18	(103)	5.312	2.115	1.7711	6.9399
	54.90	(202)	5.359	2.118	1.7928	6.9239
0.05M B doped CdSe	26.94	(002)	5.331	2.337	1.7463	6.8169
	30.12	(101)	5.368	2.492	1.6917	6.8861
	45.97	(103)	5.324	2.341	1.7322	6.8919
	55.16	(202)	5.342	2.317	1.6137	6.7935

Figure 4.4 (a-e) show XRD patterns of boron doped CdSe films with different boron concentrations at 275°C substrate temperatures. Films prepared by spray pyrolysis at 275 °C were defined by the (002), (101), (103) and (202) privileged planes. All films are orientated along (101) crystal plane at 2θ = 29.92º, 30.19º, 30.05º, 29.98º and 30.12º. This shows that the sprayed boron doped CdSe films are polycrystalline with the wurtzide hexagonal and/or cubic structure and show a good c-axis orientation

perpendicular to the substrate. The c-axis orientation in boron doped CdSe films can be concluded from "survival of the fastest" model proposed by Van der Drift [75].

This model states that at the initial stage of the film formation the nucleations with different orientations can be formed and each nucleus competes to deposite but only nuclei having the fastest growth rate can reach this c-axis orientation. It was seen from X-ray diffraction patterns, CdO phase was suggested that oxide atoms put in the place of selenium in the cubic and/or hexagonal lattice and/or oxide separated to the non-crystalline region in grain boundary. When the boron concentration increases, the 2θ value of the measured diffraction peaks do not alter importantly but the intensities of the peak of the (101) plane increases. It was the evidence of improving the crystalline properties of the films. Grain sizes become larger by increased concentration of the boron. The results in Figure 4.4 present that the crystalline properties and degree of orientation of the CdSe:B films were very associated with the boron contents and also have an important role in defining the structure of the CdSe:B films.

Figure 4.4(a-e) indicates that most of the grains in CdSe:B films have a strong orientation along (002), (101), (103) and (202) planes. While the intensity of (101) peaks increases with increase of boron concentration up to 0.01 M, then the intensity of (002), (101), (103) and (202) peaks decreases with increase of boron concentration from 0.015M to 0.05 M. The increasing in boron doping enchances the stoichiometry of the films and increases the quality of crystalline properties. It is also shown in Figure 4.4 that the formation of new nucleating centers due to the Boron atoms was resulted in the initial increase in the X-ray diffraction peaks.The succeeding reduce of the X-ray diffraction peaks for the high doping level also the decreasing crystallinity level of the films could be defined by means of two factors; first one is the newer nucleating centers are the saturated and second one is owing to the variation of the energy absorption at the time of collision.

For B-doped films, the increase in dopant contents (up to 0.01 M boron doped) results in the increases in the grain size initially. The grain size of doped films decreases for high doping level. It is observed that there was a strong dependence between the XRD intensity and the boron concentrations. The intensity of the XRD peaks was reach its maximum value when the molarity of the added boric acid is equal to 0.01 M. Thus,

the increment of the dopant level arises in a substitution in favourable growth in (002) and (101) direction. Two specified spray conditions were encountered to be optimal for the spray deposition of high quality boron doped CdSe films; first one is a substrate temperature of 275°C and second one is the concentration of boric acid of 0.01 M. It is concluded that there is a critical doping value in the starting solution. At this critical point, the characteristics of the CdSe:B films has a minimal value, grain size has maximal found for deposited films. So, the characteristics of boron doped sprayed CdSe films have identical behavior observed by Pawar et al. [76]; there was a strong dependence on the films owing to the boric acid concentrations.

Then, it is observed that when the addition of boric acid contents continues, the quality of the films decreases and also the grain size becomes smaller. And also the inreasing of the full width at half maximum (FWHM) shows us the shrinkage of the crystallinity. It may be possible that this drastic decrease in grain size is due to the large difference in ionic radius of boron. Thus, there is a decrease in the crystal grain size with the increase in the boric acid concentrations, which may be due to the sufficient increase in the satisfication of thermal energy for re-crystallization. The grain boundaires behaves as barriers for carrier transport and traps for free carrier. Also the number of the grain boundaries increases with small grain size. The decrease of crystallite size can also cause a growth of grain boundary scattering. This trend is the evidence of the creation of the newer nucleation centers by means of boron doping which in turn, would change the nucleation type from homogeneous to heterogeneous, and the crystalline structure is declined at high doping level.

The lattice constant a for the cubic phase structure is determined by the relation

$$a^2 = \frac{\lambda^2(h^2 + k^2 + l^2)}{4 Sin^2 \theta} \tag{4.1}$$

where θ is the diffraction spectra Bragg angle, λ is the wavelength of the X-ray [77]. Lattice parameters for the undoped and boron doped CdSe films are calculated using the relevant formula and tabulated in Table 4.2 The lattice constant a first decline, reaches a minimum value around undoped CdSe film and then shows a slow enhacement with increase of the boron doped around the 5.349 and 5.412 Å as shown in Table 4.2. The slow variation of lattice constant for the sprayed boron doped CdSe film over the bulk

clearly suggests that the film grains are strained which may be due to the nature and concentration of the native imperfections changing.

The change in the molar ratio of the boron in the CdSe is releated with the varying in grain size and boundary. It is observed that the XRD patterns of the undoped and boron doped CdSe films show a most preferred orientation along (002), (101), (103) and (202) planes. The grain size of all films were estimated for the planes by using the Scherrer formula [78]:

$$d = \frac{\lambda}{D\cos\theta} \qquad (4.2)$$

where d is the grain size, λ is the X-ray wavelength used, D is the angular line width of the half maximum intensity and θ is the Bragg angle. The grain parameters of the undoped and boron doped CdSe films which are associated to the (002), (101), (103) and (202) peaks are tabulated in Table 4.2. From these results, the boron concentration increases to 0.01 M concentration, the intensity of the peak of the (101) plane increases, and this peak becomes narrower indicating an enchacement of the crystallinity. This means that the grain size of the films increases with increasing up to 0.01 M concentration of the boric acid. Then the boron concentration increases from 0.015 M to 0.05 M concentration of the boric acid, the intensity of the peak of the (101) plane peaks decreases, and this peak becomes larger due to the destruction of the crystal structure and the decreasing in the grain size. The intensity of the XRD peaks depends strongly on the permitted boron concentration. Maximal XRD intensity is illustrated by the pronounced peak with dopant contents (0.01 M concentration of boric acid). It is shown that the reducing of the grain size is correlated with the extention of the XRD peak. Smaller crystallite size results in a increasing of the density of grain boundaries. Hence, a decrease in the crystallite size can cause an increase in the grain boundary scattering [79]. This observation correlates with the results of XRD patterns. The geometric mismatch at interphase boundaries between crystalline lattices of films and substrate is results in misfit stresses in the crystalline films. Therefore, it can be said that the stress is also developed in the film due to the lattice misfit [80].

However, the stress has two components: thermal stress occuring from the difference of expansion coefficient of the film and substrate and internal stress originate

from the accumulation effect of the crystallographic flows that are built into the film during deposition. The average stresses of the deposited films are due to be compressional in nature. The compressive stress is found to the grain boundary effect. The compressive stress is predominant in polycrystalline film [81]. Compressive stress is also likely to be due to the native defects setting in the lattice misfit. Native imperfections probably settle parallel to the film substrate with their surface mobility changed by the substrate temperatures. The origin of the strain is also related to the lattice misfit which results due to the the deposition conditions.

The microstrain (ε) developed in the sprayed CdSe:B films were calculated from equation [82]:

$$\varepsilon = \frac{D\cos\theta}{4} \tag{4.3}$$

where D is the full width at half maximum of the (002), (101), (103) and (202) peaks and given in Table 4.2. Table 4.2 shows the variation of the microstrain (ε) with boron concentration in CdSe:B films. It is observed from Table 4.2 for the (101) plane that the microstrain (ε) decreases with increase of the boric acid concentration up to 0.01 M. This kind of varying in microstrain may be because of the predominant recrystallization phemenon in the polycrystalline films and due to the migration of interstitial Cd atoms from inside the crystallites to its grain boundary which spread and lead to a decrease in the concentration of lattice imperfections [83].

Also it is observed that when microstrain reduces, the grain size of the films grows. This can be assigned to an enhancement in crystallinity level of the films due to the regular arrangements of atoms in the crystal lattice and which can be exhibited in the XRD results. Besides this it can be said that the microstrain reduces with the increase of boric acid concentration up to 0.01 M and then increases with the increase of boric acid concentration. It is clear from Table 4.2 that the internal microstrain within the film decreases and there is an increase in the crystallite size. Dislocations is a type of an imperfection in a crystal related with the misregistry of the lattice in one part of the crystal with respect to another part. Vacancies and interstitial atoms are in equilibrium but the dislocations are not equilibrium imperfections, i.e. thermodynamic considerations are insufficient to account for their existence in the observed densities.

In fact, the dislocations have great importance involved by the growth mechanism. In this study, the dislocation density is determined from Williamson's and Smallman's method using the following relation for undoped and boron doped CdSe films [84] and the variation of the dislocation density with boron concentration is shown in Table 4.2:

$$\rho = \frac{15\varepsilon}{aD} \tag{4.4}$$

The dislocation density (ρ) is calculated from the length of dislocation lines per unit of the crystal. As seen from Table 4.2, the dislocation density (ρ) for the plane (101) decreases with the increase of boron concentration up to (0.01 M) and then increases with the increase of boron concentration. It is clear from Table 4.2 that there occurs a decrease of a number of lattice imperfections within the film and an increase in the crystallite size. This may be due to a decrease in the occurrence of grain boundaries because of a improving in the grain size of the film with increase in boric acid concentration up to (0.01 M). These parameters show the formation of high quality boron doped CdSe films deposited on the well cleaned glass substrate by the spray pyrolysis method with dopant contents must be up to 0.01 M. This can be attributed to the increase in crystallinity due to the regular arrangements of atoms in the crystal lattice.

Therefore, it could be also due to a enhancement in the crystallinity level which leads a reduction of donor sites trapped at the dislocations and grain boundaries. Also it is understood that the grain size reduces due to the development of the dislocation density and the microstrain at the higher doping level. Since the dislocation density and the microstrain are the exhibition of dislocation network in the films, the increase in the microstrain and the dislocation density suggest the formation of lower quality films at upper boron doping level [84]. From the above results, it is concluded that boron doping plays an important role in the crystalline properties of CdSe films and effectively modifies the microstructure of the CdSe films.

4.5 Optical Studies of CdSe Films

Optical absorption analysis of the sprayed CdSe films deposited on the glass substrate at 275 $^\circ$C substrate temperature with different boron concentrations have been

carried out in the wavelength range of 300 nm to 900 nm employing a UV/VIS spectrophotometer (Jasco 7800 model). The absorption coefficient as a function of photon energy was evaluated and plotted for allowed direct transitions (neglecting exciton effects) by using the expression [85].

$$\alpha = \frac{A}{h\nu}\left(h\nu - E_g\right)^{1/2} \tag{4.5}$$

Where h is the planck constant, $\nu = c/\lambda$, c is the speed of light and λ is the wavelength of light, E_g denotes the optical band gap of the film, A is a characteristic parameter (independent of photon energy), $h\nu$ is the photon energy.
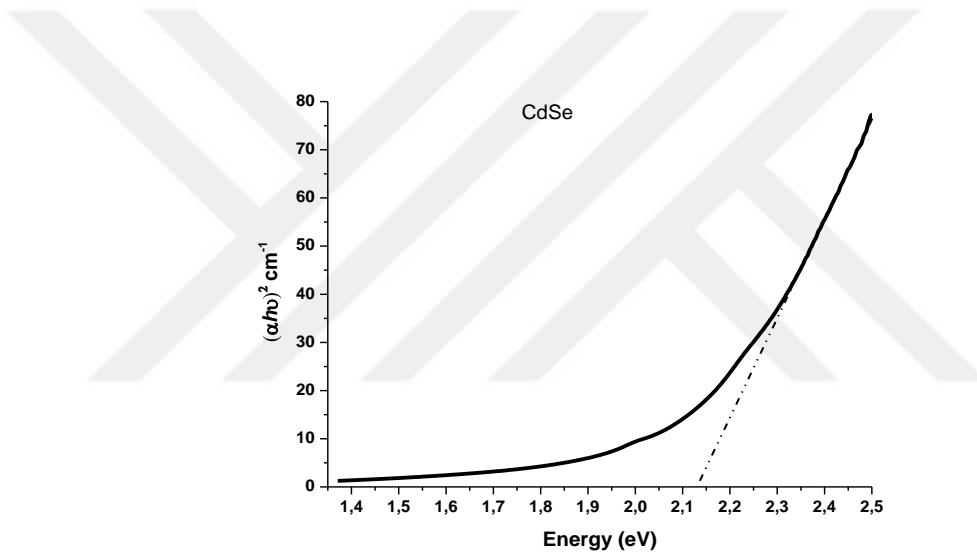
Figure 4.5 The band gap energy graph of CdSe film growth at 275 °C on glass substrate.

Figure 4.5 shows that the dependences of $(\alpha h\nu)^2$ as a function of photon energy $h\nu$ points the direct nature of band-to-band transitions for the CdSe film sample. The values of the optical band gap, E_g, has been determined by extrapolating the linear portions of respective curves to $(\alpha h\nu)^2 \to 0$. In this study, a few different samples were deposited on a high cleaned glass substrate at substrate temperature 275°C. It is seen from Figure 4.5 that the band gap energy of the CdSe film is 2.16 eV at 275°C. [27,24].

Undoped and boron doped CdSe films are direct band gap semiconductors and their absorption coefficient (α) and optical band gap energy (E_g) are inter related [85]. The band gap energy of the films was evaluated from the $(\alpha h\nu)^2$ versus $h\nu$ (photon energy) which is plotted in Figure 4.6 (a,b,c,d). The plots are parabolic in nature and the

number of inflexions reveals the number of transitions. Figure 4.6 shows that the dependences of $(\alpha h v)^2$ as a function of photon energy hv indicate the direct nature of band-to-band transitions for the considered samples with the boric acid concentration in solution with Figure 4.6 (a) 0.0025 M, (b) 0.010 M, (c) 0.015 M, (d) 0.05 M.
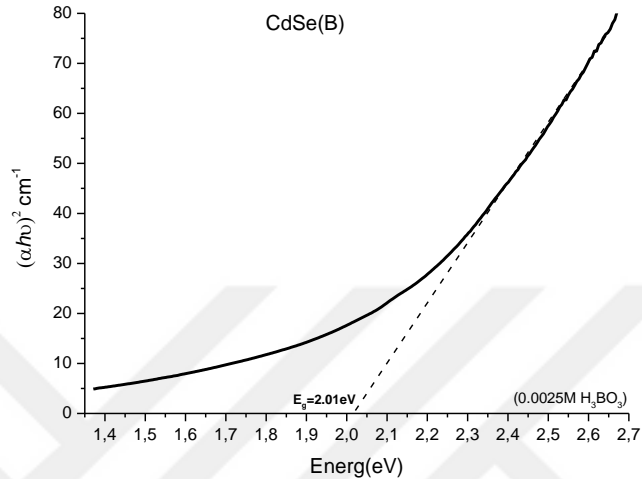
Figure 4.6 (a) The band gap energy graph of boron doped CdSe film growth at 275 °C on glass substrate.
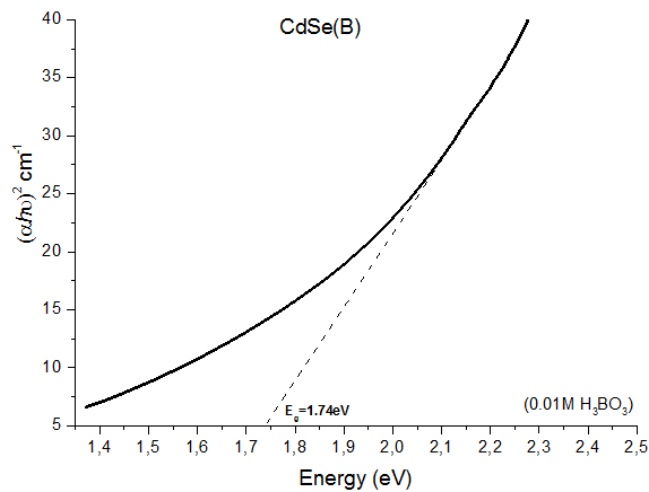
Figure 4.6 (b) The band gap energy graph of boron doped CdSe film growth at 275 °C on glass substrate.
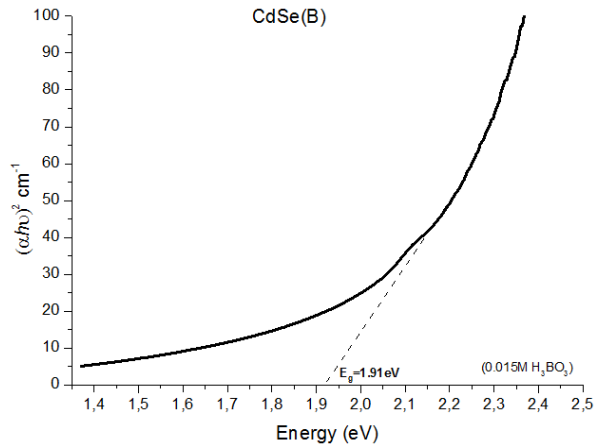
Figure 4.6 (c) The band gap energy graph of boron doped CdSe film growth at 275 °C on glass substrate.
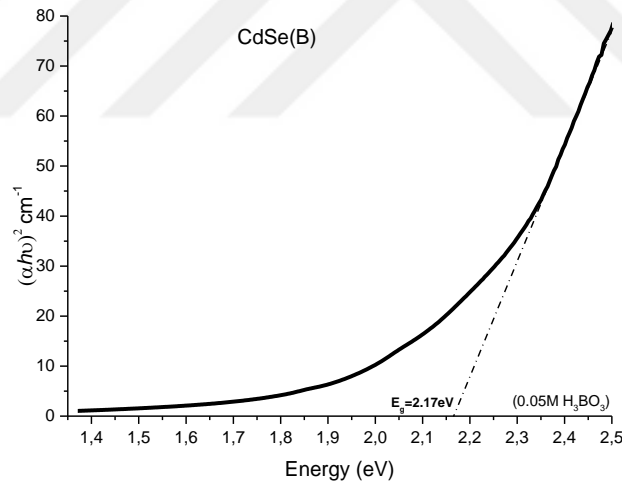
Figure 4.6 (d) The band gap energy graph of boron doped CdSe film growth at 275 °C on glass substrate.

Table 4.3 shows the optical band gap values obtained by extrapolating the linear portion of the plots of $(\alpha h\nu)^2$ versus $(h\nu)$ to $\alpha = 0$. These plots are given in Figure 4.6 for the films deposited at 275 °C substrate temperature. It is seen that the slight reduction in the optical band gap of the films with the increasing boron concentrations can be imputed to the increase in the grain size to consider the (101) plane in dopant contents (up to 0.01 M). Another reason could be the increasing in the crystallinity level with

increasing grain size. This means that the boron concentration also affects the band gap of the film. And this may be due to the extension of electronic states of the impurity phase, precipitates and clusters, into the band gap of CdSe:B. It is seen at higher doping levels that the band gap was enhanced, and the grain size of CdSe:B films was reduced. A similar behavior was observed in ZnO:Cu films deposited by spray pyrolysis method [77]. The change in Eg with the boron concentrations in solution and grain size was observed in CdSe:B films. Therefore, the band gap energy shift of CdSe:B films in our study can be imputed to the quantum size effect. The quantum size effect is observed in the films of semiconductors also it results a change in Eg with boron concentrations in solution. Therefore, the optical band gap (E_g) of doped CdSe is larger than that of undoped CdSe films. It may be also another reason that defects are accumulated at the grain boundaries. Smaller grain size results in a tensile strain because of the thermal mismatch between the CdSe film and the substrate. This indicates that the presence of large number of grain boundaries increases the defects in the film. Therefore, the change in E_g with boric acid contents can be correlated with the change of the structural properties of the films.

Table 4.3 The band gap values of boron doped and undoped CdSe films

Molarity of Boron (M)	Bandgap (eV)
0	2.17
0.0025	2.05
0.010	1.74
0.015	1.91
0.05	2.13

CHAPTER 5

CONCLUSIONS

The study of the structural, morphological and optical properties of undoped and doped CdSe films obtained by the spray pyrolysis technique at different boron doping concentrations exhibits that they are strong dependence on the boron concentration. Particularly, it is observed that the best crystallinity of CdSe films is obtained at the 275°C substarte temperature and the 0.01 M boron concentration. The films have polycrystalline structures and show a preferential orientation along (002), (103) and (202) with well-defined microstructures and it is possible that general CdSe films exist in two crystal structures, namely, Wurtzite (cubic) and zinc blende (hexagonal).

The polycrystalline structure of the CdSe films has been showed from the X-ray diffraction patterns support this property. XRD images show that the difference between these images were apparent especially those of the undoped films, where the density of grains and the grain size were larger at the boron concentration up to 0.01 M which is consistent with the pre-mentioned results of the X-ray diffraction patterns. This result is in aggrement with the behavior of the crystalline properties of the films, due to this process, resonable developments with the underlying grains do well carry on and new grains are nucleated on the top of the introducing ones. Increase in crystallinity and crystallite size with boron concentration up to 0.01M is due to the optimum rate of supply of thermal energy for recrystallization with boron contents. Also, the grain sizes of the samples increased and FWHM decreased as boron concentration up to 0.01 M, implying that the crystallization degree was improved with the rising boron contents. We expect that this increase in grain size could not continue with increasing boron contents, but it reaches a certain value after which no further increase occurs. Also, the crystallite size of all films increased initially with the increase of boron concentration and reached a maximum value at 0.01M boron concentration and became more or less constant after wards. And the reduction of grain size with the increase of strain due to the relayed

crystal growth when the stretched lattice increases the lattice energy and indicates the driving force for the grain growth in the sprayed undoped and doped CdSe films. As a result, the crystallization level is low at higher doping level (0.015 M boron concentration) due to the increasing grain boundaries which behave as defects and they affect the structural properties of the films. From the XRD and SEM analyses it was concluded that B incorporation plays an important role in the crystalline and structural properties of the sprayed CdSe films, and 0.01M boron incorporations are the most suitable boron amounts. Also, the dislocation density and microstrain were found to decrease at the boron concentration up to 0.01 M and hence grain size indicating the enhancement of CdSe films.

Generally, the energy band gap of the polycrystalline semiconductors, can be affected by the stoichiometric deviations, quantum size effect, substution in preferred orientation of the films, microstrain, dislocation density and disorder at the grain boundaries. The optical absorption studies showed that the undoped and boron doped CdSe films is direct band gap material with band gap energy around 2.17 - 1.74 eV. This behavior indicates that when the boron contents were increased, the band gap shifted to a lower energy value, which indicates that crystallization would cause the E_g narrowing. Theoretically, the reduction of optical band gaps is dealed with the volume change with temperature and electron-phonon interaction. It could be defined by crystalline state enhancement with increasing the substrate temperature. Also, the shift regarded at absorption edge toward lower photon energies for films deposited with the boron concentration up to 0.01M, could be charged to the increase in crystallite size and change in the stoichiometry due to loss of oxygen, resulting in the formation of shallow acceptor levels in the forbidden band of CdSe films. It is clearly seen that with increasing the boron concentration up to 0.01 M, the E_g of the films is broadened and the grain size increases. This is defined by the fact that the free electrons are trapped at grain boundaries. When the grain size increases, the density of grain boundaries decreases because fewer carriers are trapped in the space charge region. This process leads to a higher amount of free carriers. Then the band gap energy is increased to 2.13eV as the boron concentration was increased to 0.05M. It is implied that the energy band gaps, for CdSe films extend with increasing the boron concentration while microstrain and dislocation density increases and grain size decreases. Thus, it is concluded that the

increase in the band gap is due to the microstrain and dislocation density in the films. Also, the reduction of the energy gap by the grain size will be due to shrinkage of the quantum size effect. Also the size of the cluster of grains composed when the film deposition is so small that cause the quantum effects. From the XRD results, it is clear that the optical band gap decreases with the decrease of defects and with the increasing of crystalline property. Since microstrain is decreases the film quality because they behave as the manifestation of dislocation network in the films. The reduction in microstrain exhibits a decrease of the concentration of lattice imperfections and the formation of high quality films with increasing grain size and enhancement in the crystallinity level of films with less defects. The change of energy band gap and dislocation density with grain size could deduce that the lower the dislocation density, the lower the energy band gap. This evidences that dislocation density in the films confines the growth of grains. This may results in the retardement in crystal growth due to the stretched lattice that can increase the lattice energy and declines the driving force of the growth. As a result, the crystallite size of CdSe films can be affected form defects, impurities, microstrain, dislocation density, energy band gap and boron concentration. Thus, it can be said that the observation in decreasing of E_g, dislocation density and microstrain with increasing grain size could be ascribed to the improvement of the crystallinity.

The variations of structural, morphological and optical properties were observed depending of the dopant materials, as a consequence, boron doping to CdSe structure exhibit promise to be more suitable material than other dopants currently being used in optoelectronic device technology.

REFERENCES

[1] Perednis, D. (2003). *Thin film deposition by spray pyrolysis and the application in solid oxide fuel cells.* (Doctoral dissertation, Diss., Naturwissenschaften ETH Zürich, Nr. 15190, 2003).

[2] Mochel, J. M. (1951). *U.S. Patent No. 2,564,707*. Washington, DC: U.S. Patent and Trademark Office.

[3] Chamberlin, R. R., & Hill, J. E. (1964). *U.S. Patent No. 3,148,084*. Washington, DC: U.S. Patent and Trademark Office.

 [4] Balkenende, AR, Bogaerts, AAMB, Scholtz, JJ, Tijburg, RRM, & Willems, HX (1996). Thin MgO layers for effective hopping transport of electrons, *Philips Journal of Research*, **50(3)**, 365-373.

[5] Arya, S. P. S., & Hintermann, H. E. (1990). Growth of Y- Ba- Cu- O superconducting thin films by ultrasonic spray pyrolysis. *Thin Solid Films*, **193**, 841-846.

[6] ávan der Put, P. J. (1996). Morphology control of thin $Li\,CoO^2$ films fabricated using the electrostatic spray deposition (ESD) technique. *Journal of Materials Chemistry*, **6(5),** 765-771.

[7] Mooney, J. B., & Radding, S. B. (1982). Spray pyrolysis processing. *Annual review of materials science*, **12(1)**, 81-101.

[8] Tomar, M. S., & Garcia, F. J. (1981). Spray pyrolysis in solar cells and gas sensors. *Progress in Crystal Growth and Characterization*, **4**(3), 221-248.

[9] Albin, D. S., & Risbud, S. H. (1987). Spray pyrolysis processing of optoelectronic materials. *Advanced Ceramic Materials;(USA)*, **2(3A).**

[10] Pamplin, B. R. (1979). Spray pyrolysis of ternary and quaternary solar cell materials. *Progress in Crystal Growth and Characterization*, **1(4)**, 395-403.

[11] Patil, P. S. (1999). Versatility of chemical spray pyrolysis technique. *Materials Chemistry and physics*, **59(3)**, 185-198.

[12] Schoonman, J., & Riess, I. (2000). *Oxygen ion and mixed conductors and their technological applications* **(Vol. 368)**. Springer Science & Business Media.

[13] Perednis, D., & Gauckler, L. J. (2005). Thin film deposition using spray pyrolysis. *Journal of electroceramics*, **14(2)**, 103-111.

[14] Baban C., G.I., Rusu P. Prepelita, 2005. J. Optoelectronics Adv. Mater. **7**, 817.

[15] Licht, S., & Peramunage, D. (1990). Efficient photoelectrochemical solar cells from electrolyte modification.

[16] Murali K R, Subramanian V, Rangarajan N, Lakshmanan A S and Rangarajan S K 1993 Bull. Electrochem. **9(209)**.

[17] Kainthla, R. C., Pandya, D. K., & Chopra, K. L. (1982). Photo-electronic properties of solution-grown CdSe films. *Solid-State Electronics*, **25(1)**, 73-76.

[18] Reichman, J., & Russak, M. A. (1982). Improved efficiency of n-CdSe thin-film photoelectrodes by zinc surface treatment. *Journal of Applied Physics*, **53(1)**, 708-711.

[19] Murali, K. R., Subramanian, V., Rangarajan, N., Lakshmanan, A. S., & Rangarajan, S. K. (1991). Photoelectrochemical studies on pulse plated CdSe films. *Journal of electroanalytical chemistry and interfacial electrochemistry*, **303(1)**, 261-266.

[20] Elango. T, Subramanian. V, Murali. K. R. (2000). Characteristics of spray-deposited CdSe thin films, Surface and Coatings Technology. **123**. 8–11.

[21] Ubale, A. U., & Ibrahim, S. G. (2015). Structural, electrical and optical properties of nanocrystalline Cd 1− xFexSe thin films deposited by chemical spray technique. *Journal of Saudi Chemical Society*, **19(6)**, 667-675.

[22] Logu, T., Sankarasubramanian, K., Soundarrajan, P., & Sethuraman, K. (2015). Hydrophilic CdSe thin films by low cost spray pyrolysis technique and annealing effects. *Electronic Materials Letters*, **11(2)**, 206-212.

[23] Logu T., Sankarasubramanian K., Soundarrajan P., Sampath M., Sethuraman K., Hydrophobic, 2013. Cdse: Sb Thin Films by Chemical Spray Pyrolysis Technique, *International Journal of Science and Research (IJSR),* ISSN (Online): 2319-7064, Impact Factor: 4.438, 36-39.

[24] RI Chowdhury, MS Islam, F Sabeth, G Mustafa, SFU Farhad, DK Saha, FA Chowdhury, S Hussain, ABMO Islam, (2012). Characterization of Electrodeposited Cadmium Selenide Thin Films., Dhaka University Journal of Science. **60(1)**: 137-140.

[25] Kale, R. B., & Lokhande, C. D. (2004). Influence of air annealing on the structural, optical and electrical properties of chemically deposited CdSe nano-crystallites. *Applied Surface Science*, **223(4)**, 343-351.

[26] Lade, S. J., Uplane, M. D., Uplane, M. M., & Lokhande, C. D. (1998). Structural, optical and photoelectrochemical properties of electrodeposited CdSe thin films. *Journal of materials science: Materials in electronics*, **9(6)**, 477-482.

[27] Betkar, M. M., & Bagde, G. D. (2012). Structural and optical properties of spray deposited CdSe Thin films. *Materials Physics and Mechanics*, **14**, 74-77.

[28] Gudage, Y. G., Deshpande, N. G., & Sharma, R. (2009). Influence of pH on microstructural and optical properties of electrosynthesized CdSe thin films. *Journal of Physics and Chemistry of Solids*, **70(6)**, 907-915.

[29] Yadav, A. A., Barote, M. A., & Masumdar, E. U. (2010). Studies on cadmium selenide (CdSe) thin films deposited by spray pyrolysis. *Materials Chemistry and Physics*, **121(1)**, 53-57.

[30] Kariper I. A.(2016). Optical and structural properties of cdse thin film produced by chemical bath deposition. *Journal Non-Oxide Glasses*. **8**, 1-9.

[31] Zhao, Y., Yan, Z., Liu, J., & Wei, A. (2013). Synthesis and characterization of CdSe nanocrystalline thin films deposited by chemical bath deposition. *Materials Science in Semiconductor Processing*, **16(6)**, 1592-1598.

[32] Mahato, S., Shakti, N., & Kar, A. K. (2015). Annealing temperature dependent structural and optical properties of electrodeposited CdSe thin films. *Materials Science in Semiconductor Processing*, **39**, 742-747.

[33] Purohit, A., Chander, S., Nehra, S. P., & Dhaka, M. S. (2015). Effect of air annealing on structural, optical, morphological and electrical properties of thermally evaporated CdSe thin films. *Physica E: Low-dimensional Systems and Nanostructures*, **69**, 342-348.

[34] Huş, Ş. M., & Parlak, M. (2008). Electrical, photo-electrical, optical and structural properties of CdSe thin films deposited by thermal and e-beam techniques, *Journal of Physics D: Applied Physics*, **41(3)**, 035405.

[35] Kale, R. B., & Lokhande, C. D. (2004). Band gap shift, structural characterization and phase transformation of CdSe thin films from nanocrystalline cubic to nanorod hexagonal on air annealing. *Semiconductor Science and Technology*, **20(1)**, 1.

[36] Mansour, H. L., Mishjil, K. A., Habubi, N. F., & Chiad, S. S. (2014). Structural and Optical Properties of Cd^ sub 0.4^ Se^ sub 0.6^ Thin Films Prepared by CBD. *International Journal of Thin Films Science and Technology*, **3(2)**, 57.

[37] Lee, J. H., Yi, J. S., Yang, K. J., Park, J. H., & Oh, R. D. (2003). Electrical and optical properties of boron doped CdS thin films prepared by chemical bath deposition. *Thin Solid Films*, **431**, 344-348.

[38] Altosaar, M., Ernits, K., Krustok, J., Varema, T., Raudoja, J., & Mellikov, E. (2005). Comparison of CdS films deposited from chemical baths containing different doping impurities. *Thin solid films*, **480**, 147-150.

[39] Bedir, M., Öztaş, M., & Kara, H. (2013). Effect of the substrate temperature on the structural, optical and electrical properties of spray-deposited CdS: B films. *Journal of Materials Science: Materials in Electronics*, **24(2)**, 499-506.

[40] Khallaf, H., Chai, G., Lupan, O., Chow, L., Heinrich, H., Park, S., & Schulte, A. (2009). In-situ boron doping of chemical-bath deposited CdS thin films. *Physica status solidi (a)*, **206(2)**, 256-262.

[41] Yan, L. L., Wang, X. B., Liu, W. K., & Li, X. J. (2015). Effect of boron doping on the rectification effect and photovoltaic performance of CdS/Si heterostructure based on Si nanoporous pillar array. *Journal of Physics D: Applied Physics*, **48(26)**, 265101.

[42] Lee H.Y., Lee J. H., Kim J. H., Seo K. S. and Park Y. K. (1998). Proc. Int. Conf. Electrical Engineering, Kyonju, p. 877.

[43] Lee, J. H., Lee, H. Y., Kim, J. H., & Park, Y. K. (2000). Heat treatment of boron-doped CdS films prepared by chemical bath deposition for solar cell applications. *Japanese Journal of Applied Physics*, **39(4R)**, 1669.

[44] Koinkara P. M., Yonekura D. (*2009).* Field emission investigation of boron doped diamond thin films synthesized by microwave plasma chemical vapor depositio: Effect of vacuum annealing, *Techinical Digest of IVNC.*

[45] Hao, X. J., Cho, E. C., Flynn, C., Shen, Y. S., Conibeer, G., & Green, M. A. (2008). Effects of boron doping on the structural and optical properties of silicon nanocrystals in a silicon dioxide matrix. *Nanotechnology*, **19(42)**, 424019.

[46] Li, W., Li, Y., Du, G., Chen, N., Liu, S., Wang, S., & Niu, X. (2016). Enhanced electrical and optical properties of boron-doped ZnO films grown by low pressure chemical vapor deposition for amorphous silicon solar cells. *Ceramics International*, **42(1)**, 1361-1365.

[47] Novruzov, V. D., Keskenler, E. F., Tomakin, M., Kahraman, S., & Gorur, O. (2013). Effects of ultraviolet light on B-doped CdS thin films prepared by spray pyrolysis method using perfume atomizer. *Applied Surface Science*, **280**, 318-324.

[48] Lee, J. (2004). Raman scattering and photoluminescence analysis of B-doped CdS thin films. *Thin Solid Films*, **451**, 170-174.

[49] Streetman, B. G. and Banerjee, S. K. (2006). Solid state Electronic Devices, 6th Ed., Prentice-Hall, Inc., New Delhi, ISBN 978-81 -203-3020-7.

[50] Neamen, D. A. (2001). Semiconductor physics and devices: Basic principles, 3rd Ed., McGraw-Hill, Inc., New York, ISBN 0-07-232 107-5.

[51] Grundmann, M. (2010). The Physics of Semiconductors: An Introduction Including Nanophysics and Applications (Graduate Texts in Physics).

[52] Freund, L. B., & Suresh, S. (2004). *Thin film materials: stress, defect formation and surface evolution*. Cambridge University Press.

[53] Yacobi, B. G. (2003). *Semiconductor materials: an introduction to basic principles*. Springer Science & Business Media.

[54] Sheng S. Li, 2006, Semiconductor Physical Electronics Second Edition, Springer Science+Business Media, LLC, ISBN **13**: 978-0387-28893-2.

[55] Callister Jr, W. D. (2001). Fundamentals of Materials Science and Engineering John Wiley & Sons. *Inc., New York,* **524 *p***.

[56] Ayvazian, T. (2013). *Electrical and Optical Characterization of Nanowire based Semiconductor Devices*.

[57] Hone, F. G. (2015). *Synthesis and characterization of cadmium selenide (Cdse) and lead sulphur selenide (Pbs1-Xsex) thin films by chemical bath deposition method* (Doctoral dissertation, Department of Physics, Kwame Nkrumah University of Science and Technology).

[58] C. Ghezzi, R. Magnanini, A. Parisini, B. Rotelli and L. Tarricone. (1995). Optical absorption near the fundamental absorption edge in GaSb. Physical Review B. **52.** 1463-1466.

[59] Sahoo, S., Chakraborti, C. K., Mishra, S. C., & Nanda, U. N. (2011). Scanning Electron Microscopy as an analytical tool for particle size distribution and aspect ratio analysis of Ciprofloxacin Mucoadhesive Polymeric suspension.

[60] Rau, U., Abou-Ras, D., & Kirchartz, T. (Eds.). (2011). *Advanced characterization techniques for thin film solar cells*. John Wiley & Sons.

[61] Garratt-Reed A.J. and Bell D.C. 2005 Energy-Dispersive X-Ray Analysis in the Electron Microscope, this edition published in the Taylor & Francis e-Library, ISBN 0-203-53754-8 Master e-book ISBN.

[62] Pool, Charles P., Ovens, Frank J. (2003). Introduction to Nanotechnology. John Wiley and Sons. ISBN 0-471-07935-9.

[63] Servati, P., Colli, A., Hofmann, S., Fu, Y. Q., Beecher, P., Durrani, Z. A. K. & Milne, W. I. (2007). Scalable silicon nanowire photodetectors. *Physica E: Low-dimensional Systems and Nanostructures*, **38(1)**, 64-66.

[64] Konstantatos, G., Levina, L., Fischer, A., & Sargent, E. H. (2008). Engineering the temporal response of photoconductive photodetectors via selective introduction of surface trap states. *Nano letters*, **8(5)**, 1446-1450.

[65] Banfi, G., Degiorgio, V., & Tan, H. M. (1995). Optical nonlinearity of semiconductor-doped glasses at frequencies below the band gap: the role of free carriers. *JOSA B*, **12(4)**, 621-628.

[66] Shyju, T. S., Anandhi, S., Indirajith, R., & Gopalakrishnan, R. (2011). Solvothermal synthesis, deposition and characterization of cadmium selenide (CdSe) thin films by thermal evaporation technique. *Journal of Crystal Growth*, **337(1)**, 38-45.

[67] Gnatenko, Y. P., Bukivskij, P. M., Faryna, I. O., Opanasyuk, A. S., & Ivashchenko, M. M. (2014). Photoluminescence of high optical quality CdSe thin films deposited by close-spaced vacuum sublimation. *Journal of Luminescence*, **146**, 174-177.

[68] Li, sheng. (2006) *Semiconductor physical electronics* (2nd ed.) Springer. ISBN:978-0-387-28893-7.

[69] Girtan, M., & Folcher, G. (2003). Structural and optical properties of indium oxide thin films prepared by an ultrasonic spray CVD process. *Surface and coatings Technology*, **172(2)**, 242-250.

[70] Srivastava, P., & Singh, K. (2012). Synthesis of CdSe nanoparticles by solvothermal route: Structural, optical and spectroscopic properties. *Adv. Mat. Lett*, **3(4)**, 340-344.

[71] JCPDS Data Card no. 77-2307.

[72] JCPDS Data Card no. 78-0653.

[73] Ramalingam, G., & Madhavan, J. (2011). Investigation on the structural and morphological behaviour of CdSe nanoparticles by hydrothermal method. *Archives of Applied Science Research*, **3(3)**, 217-224.

[74] Deng, Z., Cao, L., Tang, F., & Zou, B. (2005). A new route to zinc-blende CdSe nanocrystals: mechanism and synthesis. *The Journal of Physical Chemistry B*, **109(35)**, 16671-16675.

[75] Van der Drift, A. (1967). Evolutionary selection, a principle governing growth orientation in vapour-deposited layers. *Philips Res. Rep*, **22(3)**, 267-288.

[76] Pawar, B. N., Jadkar, S. R., & Takwale, M. G. (2005). Deposition and characterization of transparent and conductive sprayed ZnO: B thin films. *Journal of Physics and Chemistry of Solids*, **66(10)**, 1779-1782.

[77] Öztas, M., & Bedir, M. (2008). Thickness dependence of structural, electrical and optical properties of sprayed ZnO: Cu films. *Thin Solid Films*, **516(8)**, 1703-1709.

[78] Kim, K. J., & Park, Y. R. (2004). Sol–gel growth and structural and optical investigation of manganese-oxide thin films: structural transformation by Zn doping. *Journal of crystal growth*, **270(1)**, 162-167.

[79] Bedir, M., Öztaş, M., Çelik, S. S., & ÖZDEMİR, T. (2014). Effect of Boric Acid Content on the Structural and Optical Properties of MnS Films Prepared by Spray Pyrolysis Technique. *Acta Physica Polonica, A.*, **126(3)**.

[80] Ovid ko, I. A. (2000). Interfaces and misfit defects in nanostructured and polycrystalline films. *REVIEWS ON ADVANCED MATERIALS SCIENCE*, **1**, 61-107.

[81] IH Khan, LI Maissel, R Glang, (1970). Handbook of Thin Film Technology. Mc-Grow Hill Co., New York,

[82] Bedir, M., Öztaş, M., Bakkaloğlu, Ö. F., & Ormanci, R. (2005). Investigations on structural, optical and electrical parameters of spray deposited ZnSe thin films with different substrate temperature. *The European Physical Journal B-Condensed Matter and Complex Systems*, **45(4)**, 465-471.

[83] Kröger, F. A. (1964). FA Kröger The Chemistry of Imperfect Crystals.

[84] Begum, N. J., & Ravichandran, K. (2013). Effect of source material on the transparent conducting properties of sprayed ZnO: Al thin films for solar cell applications. *Journal of Physics and Chemistry of Solids*, **74(6)**, 841-848.

[85] Heavens, O. S. (1991). Optical properties of thin solid films. Courier Corporation.